

Synchronization of a class of cyclic discrete-event systems describing legged locomotion

G.A.D. Lopes, B. Kersbergen, B. De Schutter, T.J.J. van den Boom, and R. Babuška

Abstract

It has been shown that max-plus linear systems are well suited for applications in synchronization and scheduling, such as the generation of train timetables, manufacturing, or traffic. In this paper we show that the same is true for multi-legged locomotion. In this framework, the max-plus eigenvalue of the system matrix represents the total cycle time, whereas the max-plus eigenvector dictates the steady-state behavior. Uniqueness of the eigenstructure also indicates uniqueness of the resulting behavior. For the particular case of legged locomotion, the movement of each leg is abstracted to two-state circuits: swing and stance (leg in flight and on the ground, respectively). The generation of a gait (a manner of walking) for a multiple legged robot is then achieved by synchronizing the multiple discrete-event cycles via the max-plus framework. By construction, different gaits and gait parameters can be safely interleaved by using different system matrices. In this paper we address both the transient and steady-state behavior for a class of gaits by presenting closed-form expressions for the max-plus eigenvalue and max-plus eigenvector of the system matrix and the coupling time. The significance of this result is in showing guaranteed robustness to perturbations and gait switching, and also a systematic methodology for synthesizing controllers that allow for legged robots to change rhythms fast.

Index Terms

Discrete-event systems, max-plus algebra, coupling time, legged locomotion, gait generation, robotics

I. INTRODUCTION

Synchronization of cyclic processes is important in many fields, including manufacturing [51], transportation [31], genomics [48], and neuroscience [34, 50], etc (see references within [13]). In this paper we focus on a class of multiple concurrent two-state cyclic systems with a direct application to legged locomotion. Our motivation is the requirement of legged mobile robots to cope with unstructured terrains in a flexible way by smoothly and effectively switching between different gaits.

Corresponding author G.A.D. Lopes. Tel. +31-15-2785489. All authors are with the Delft Center for Systems and Control, Delft University of Technology, The Netherlands, e-mail: {g.a.delgadolopes, b.kersbergen, a.j.j.vandenboom, b.deschutter, r.babuska}@tudelft.nl

Manuscript received xxxxxx, 20xx; revised xxxxx, 20xx.

Legged systems are traditionally modeled using cross-products of circles in the phase space of the set of continuous time gaits. Holmes et al. [34] give an extensive review of dynamic legged locomotion. The central pattern generator [35] approach to design motion controllers lies in assembling sets of error functions to be minimized that cross-relate the phases of multiple legs, resulting in attractive limit cycles for the desired gait. Switching gaits online is typically not addressed since in the central pattern generator framework switching must be modeled as a hybrid system. Additionally, implementing “hard constraints” on the configuration space [29] can be quite complex mainly due to the combinatorial nature of the gait space, and often it comes at the cost of dramatically increasing the complexity of the controller.

As an alternative to the common continuous time modeling approach, we introduce an abstraction to represent the combinatorial nature of the gait space for multi-legged robots into ordered sets of leg index numbers. This abstraction combined with max-plus linear equations allows for systematic synthesis and implementation of motion controllers for multi-legged robots where gait switching is natural and the translation to continuous-time motion controllers is straightforward [38]. The methodology presented is particularly relevant for robots with four, six, or higher numbers of legs where the combinatorial nature of the gait space starts to play an important role. For a large number of legs it is not obvious in which order each leg should be in swing or in stance. Most legged animals, in particular large mammals, are known to walk and run with various gaits on a daily basis, depending on the terrain or how fast they need to move. The discrete-event framework presented in this paper enables the same behavior for multi-legged robots. Mathematical properties are derived for this framework, giving extra insight into the resulting robot motion.

The main mathematical representation employed in this paper are switching max-plus linear equations. By defining the state variables to represent the time at which events occur, systems of linear equations in the *max-plus algebra* [1, 11, 32] can model a class of timed discrete-event systems. Specifically, max-plus linear systems are equivalent to (timed) Petri nets [44] where all places have a single incoming and a single outgoing arc. Max-plus linear systems inherit a large set of analysis and control synthesis tools thanks to many parallels between the max-plus-linear systems theory and the traditional linear systems theory. Discrete-event systems that enforce synchronization can be modeled in this framework. Max-plus algebra has been successfully applied to railroads [3, 31], queuing systems [30], resource allocation [19], and recently to image processing [2] and legged locomotion [38, 39].

The contributions of this paper are the following: we present a class of max-plus linear systems that realize the synchronization of the legs of a robot. Next, we derive closed-form expressions for the max-plus eigenvalue and eigenvector of the system matrix, and show that the max-plus eigen-parameters are max-plus unique, implying a unique steady-state behavior. This result is then used to compute the coupling

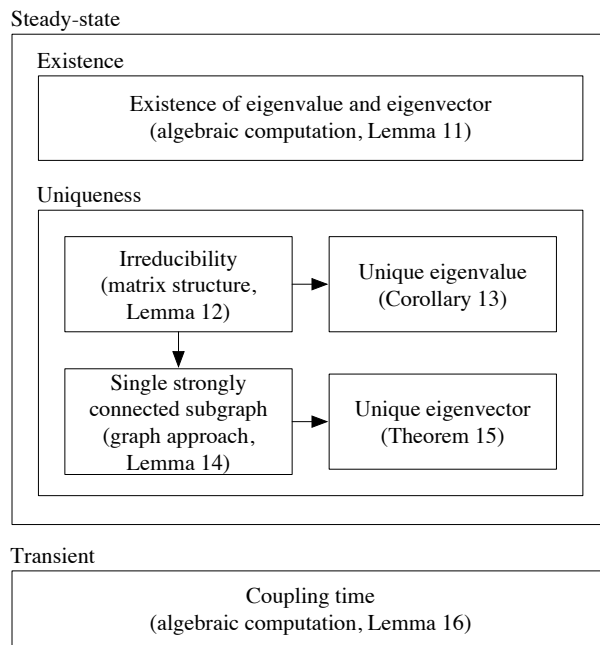


Fig. 1. Structure of the contributions of this paper. We analyze both the steady-state and the transient behavior of a class of cyclic discrete-event systems that are well suited to model legged locomotion.

time, which characterizes the transient behavior. The importance of having closed-form expressions and uniqueness of the max-plus eigen-structure is that, not only can one compute these parameters very fast without recurring to simulations or numerical algorithms (e.g. Karp’s algorithm [1]), but one has also guarantees of uniqueness: the motion of the robot will always converge in a finite number of steps to the same prescribed behavior, regardless of gait changes or disturbances. This reassurance is fundamental when designing gait controllers for robotics. Additionally we present a low least number of steps needed to reach steady-state motion after changing gaits. This paper is focused on the general mathematical properties of a class of discrete-event systems that describe legged locomotion, and not on the actual implementation of gait controllers for robots, as presented previously in [38].

In Section II we revisit the fundamentals of legged locomotion with special emphasis on gait generation and show that max-plus algebra can be used in the modeling of the synchronization of multiple legs. In Section III we briefly review relevant concepts from the theory of max-plus algebra and in Section IV we present a class of parameterizations for the gait space. Given such class, we derive a number of properties, such as the max-plus eigen-structure of the system matrices (Section IV-C), their graph representation (Section IV-D), and the coupling time (Section IV-E). Figure 1 illustrates the structure of the contributions presented in this paper.

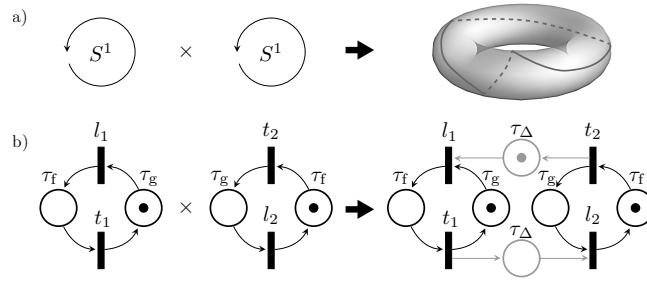


Fig. 2. Modeling of legged locomotion. a) The configuration space of two oscillators is a torus. Synchronization is achieved by constructing attractive limit cycles, represented by the curve on the torus. b) Discrete-event representations of multiple circuits can be modeled as concurrent cyclic Petri nets. Synchronization is achieved by adding extra places, represented by s_1 and s_2 .

II. MODELING LEGGED LOCOMOTION

In literature [14, 28, 34, 45, 46], the study of legged locomotion is approached from two main directions: the signal generation side, where emphasis is placed on the classes of signals that result in periodic locomotion behavior independent of the physical platform; and the mechanics side, where the (hybrid) Newtonian mechanics models are analyzed independently of the driving control signal. We focus on the first approach, by restating the traditional view of periodic gaits for legged systems being defined in the n -torus: Cartesian products of circles each representing an abstract phase that parameterizes the position of each leg in the Euclidean space. Such an abstraction serves as a platform for the models of “networks of phase oscillators” and central pattern generators, introduced in the earlier works of Grillner [27] and Cohen et al. [5]. These are now accepted by both biology and robotics communities as standard modeling tools [34].

In this paper we abstract beyond the notion of a continuous phase to consider concurrent circuits of discrete events. Taking a Petri net modeling approach, during ground locomotion the places represent leg stance (when the foot is touching the ground and supporting the body) and leg swing (when the foot and all parts of the leg are in the air). The transitions represent leg touchdown and lift off. This labeling is most convenient for ground locomotion, but one should be aware that the framework presented in this paper is valid for other types of locomotion where the phases of the various limbs need to be synchronized, such as swimming or flight. Figure 2 illustrates the conceptual difference between our approach (Figure 2.b) where each phase is represented by a circuit in the discrete-event systems domain and the traditional continuous phase central pattern generator (Figure 2.a). Here, phase synchronization is enforced on the torus by implementing controllers that achieve stable limit cycles [37]. In this paper we translate timed event graphs¹ into the equivalent representation as max-plus linear systems, and achieve synchronization

¹We restrict ourselves to a class of timed Petri nets called *timed event graphs* such that a one-to-one translation to max-plus linear systems is possible (see [32], chapter 7). In timed event graphs each place can have one single incoming arc and one single outgoing arc.

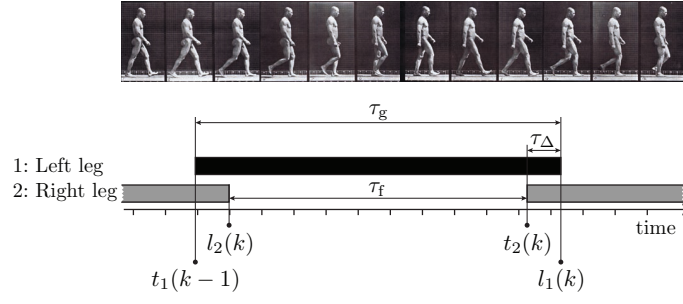


Fig. 3. Illustration of a walking pattern, photos by Muybridge [40]. The solid bars, following Hildebrand’s diagram notation [33], indicate that the leg is in stance (foot touching the ground) for τ_g time units, and white space that the leg is in swing (foot in flight) for τ_f time units. The time length when both feet are touching the ground is called the double-stance time τ_Δ . We use the notation $t_1(k-1)$ to represent the time instant when leg 1 (left leg) touches the ground, and $l_1(k)$ when it initiates a swing. The parameter k is the “step counter”.

by designing the system matrices appropriately. Consider the leg synchronization of a biped robot. In this case, only two legs need to be synchronized during locomotion. For a typical walking motion (no aerial phase) the left leg should only lift off the ground after the right leg has touched down, to make sure the robot does not fall due to lack of support. This simple synchronization requirement can be captured by introducing state variables for the transition events defined as follows: let $l_i(k)$ be the time instant leg i lifts off the ground and $t_i(k)$ be the time instant it touches the ground, both for k -th iteration, where k is considered to be a global event or “step” counter. Enforcing that the time instant when the leg touches the ground must equal the time instant it lifted off the ground for the last time plus the time it is in swing (denoted τ_f) is realized by:

$$t_i(k) = l_i(k) + \tau_f. \quad (1)$$

A similar relation can be derived for the lift off time:

$$l_i(k) = t_i(k-1) + \tau_g, \quad (2)$$

where τ_g is the stance time and $t_i(k-1)$ refers to the previous iteration such that equations (1) and (2) can be used iteratively. For this system we have that $\tau_f > 0$ and also $\tau_g > 0$. Synchronization of the cycles of two legs can be achieved by introducing a double stance time parameter, denoted τ_Δ , representing that after each leg touchdown both legs must stay in stance for at least τ_Δ time units (see Figure 3). This is captured by the following equations:

$$l_1(k) = \max(t_1(k-1) + \tau_g, t_2(k-1) + \tau_\Delta) \quad (3)$$

$$l_2(k) = \max(t_2(k-1) + \tau_g, t_1(k) + \tau_\Delta) \quad (4)$$

Equation (3) enforces simultaneously that leg 1 stays at least τ_g time units in stance and will only lift off at least τ_Δ time units after leg 2 has touched down. When both conditions are satisfied, lift off takes place.

Equation (4) is analogous for leg 2. Note that the parameters τ_f , τ_g , and τ_Δ are in fact the *minimal* swing, stance, and double stance times, respectively, as opposed to the exact times. Note additionally that these equations are non-linear but they rely only on the “max” and “plus” operations. This motivates the use of the theory of the max-plus algebra to find parsimonious discrete-event models for legged locomotion. Although the previous set of equations were designed for a walking behavior with no aerial phases, in practice they can also be used for running by choosing the double stance time to be negative, i.e. by enforcing that one leg lifts off τ_Δ time units before the other leg touches the ground. However, the results presented in this paper focus on the case when $\tau_\Delta \geq 0$ such that stability (in the sense of ensuring a desired minimum number of legs on the ground simultaneously) is guaranteed.

III. MAX-PLUS ALGEBRA

In the early sixties the fact that certain classes of discrete-event systems can be described by models using the operations \max and $+$ has been discovered independently by a number of researchers, among whom Cuninghame-Green [9, 10] and Giffler [21–23]. These discrete-event systems are called max-plus-linear systems since the model that describes their behavior becomes “linear” when formulated in the max-plus algebra [1, 11, 32], which has maximization and addition as its basic operations. More specifically, discrete-event systems in which only synchronization and no concurrency or choice occur can be modeled using the operations maximization (corresponding to synchronization: a new operation starts as soon as all preceding operations have been finished) and addition (corresponding to the duration of activities: the finishing time of an operation equals the starting time plus the duration). Some examples of max-plus linear discrete-event systems are production systems, railroad networks, urban traffic networks, queuing systems, and array processors [1, 11, 32].

An account of the pioneering work of Cuninghame-Green on max-plus system theory has been given in [11]. Related work has been done by Gondran and Minoux [24–26]. In the eighties the topic attracted new interest due to the research of Cohen, Dubois, Moller, Quadrat, Viot [6–8], Olsder [41–43], and Gaubert [15–17], which resulted in the publication of [1]. Since then, several other researchers have entered the field. For an historical overview we refer the interested reader to [12, 20, 32]. In this section we give an introduction to the max-plus algebra. This section is based on [1, 11], where a complete overview of the max-plus algebra can be found. The basic operations of the max-plus algebra are maximization and addition, which will be represented by \oplus and \otimes respectively $x \oplus y = \max(x, y)$ and $x \otimes y = x + y$, for $x, y \in \mathbb{R}_{\max} := \mathbb{R} \cup \{-\infty\}$. The zero element for \oplus in \mathbb{R}_{\max} is $\varepsilon := -\infty$ and the unit element for \otimes is $e := 0$. The structure $(\mathbb{R}_{\max}, \oplus, \otimes)$ is called the max-plus algebra [1, 11]. The operations \oplus and \otimes are called the max-plus-algebraic addition and max-plus-algebraic multiplication respectively since many properties and concepts from linear algebra can be translated to the max-plus algebra by replacing $+$

by \oplus and \times by \otimes . The max-plus algebra is a typical example of a class of algebraic structures called commutative dioids. In a dioid the additive operation \oplus is associative, commutative, and idempotent, and it has a zero element; the multiplicative operation \otimes is commutative and associative and it has an identity element; the additive zero element is absorbing for \otimes ; and \otimes is left and right distributive w.r.t. \oplus . Let $r \in \mathbb{R}$. The r th max-plus power of $x \in \mathbb{R}$ is denoted by $x^{\otimes r}$ and corresponds to rx in conventional algebra. If $x \in \mathbb{R}$ then $x^{\otimes 0} = 0$ and the inverse element of x w.r.t. \otimes is $x^{\otimes -1} = -x$. There is no inverse element for ε since ε is absorbing for \otimes . If $r > 0$ then $\varepsilon^{\otimes r} = \varepsilon$. If $r < 0$ then $\varepsilon^{\otimes r}$ is not defined. In this paper we have $\varepsilon^{\otimes 0} = 0$ by definition. The rules for the order of evaluation of the max-plus operators are similar to those of conventional algebra. So max-plus power has the highest priority, and max-plus multiplication \otimes has a higher priority than max-plus addition \oplus . Throughout this paper the i, j element of a matrix A is denoted by $[A]_{ij}$. The matrix $\mathcal{E}_{m \times n}$ is the m by n max-plus zero matrix: $[\mathcal{E}_{m \times n}]_{ij} = \varepsilon$ for all i, j . The matrix E_n is the n by n max-plus identity matrix: $[E_n]_{ii} = e$ for all i and $[E_n]_{ij} = \varepsilon$ for all i, j with $i \neq j$. We also define the m by n max-plus “one” matrix $\mathbb{1}_{m \times n}$ such that $[\mathbb{1}]_{ij} = e = 0$ for all i, j . If the dimensions of \mathcal{E} , E , $\mathbb{1}$ are omitted in this paper, they should be clear from the context. The basic max-plus-algebraic operations are extended to matrices as follows. If $A, B \in \mathbb{R}_{\max}^{m \times n}$, $C \in \mathbb{R}_{\max}^{n \times p}$ then

$$[A \oplus B]_{ij} = [A]_{ij} \oplus [B]_{ij} = \max([A]_{ij}, [B]_{ij}) \quad (5)$$

$$[A \otimes C]_{ij} = \bigoplus_{p=1}^n [A]_{ip} \otimes [C]_{pj} = \max_{p=1, \dots, n} ([A]_{ip} + [C]_{pj}) \quad (6)$$

for all i, j . Note the analogy with the definitions of matrix sum and product in conventional linear algebra. The max-plus product of the scalar $\alpha \in \mathbb{R}_{\max}$ and the matrix $A \in \mathbb{R}_{\max}^{m \times n}$ is defined by $[\alpha \otimes A]_{ij} = \alpha \otimes [A]_{ij}$ for all i, j . The max-plus matrix power of $A \in \mathbb{R}_{\max}^{n \times n}$ is defined as follows: $A^{\otimes 0} = E_n$ and $A^{\otimes p} = A \otimes A^{\otimes p-1}$ for $p \geq 1$.

Theorem 1 (see [1], Th 3.17). *Consider the following system of linear equations in the max-plus algebra:*

$$x = A \otimes x \oplus b \quad (7)$$

with $A \in \mathbb{R}_{\max}^{n \times n}$ and $b, x \in \mathbb{R}_{\max}^{n \times 1}$. Now let

$$A^* := \bigoplus_{p=0}^{\infty} A^{\otimes p} . \quad (8)$$

If A^* exists then

$$x = A^* \otimes b \quad (9)$$

solves the system of max-plus linear equations (7)

Definition 2. The matrix $A \in \mathbb{R}_{\max}^{n \times n}$ is called *nilpotent* if there exists a finite positive integer p_0 such that for all integers $p \geq p_0$ we have $A^{\otimes p} = \mathcal{E}$.

It is easy to verify that if $A \in \mathbb{R}_{\max}^{n \times n}$ is nilpotent then $p_0 \leq n$. For $A, B \in \mathbb{R}_{\max}^{n \times m}$ we say that A *overcomes* B , written as $A \geq B$ if $A \oplus B = A$ (i.e., $[A]_{ij} \geq [B]_{ij}$ for all i, j). A directed graph \mathcal{G} is defined as an ordered pair $(\mathcal{V}, \mathcal{A})$, where \mathcal{V} is a set of vertices and \mathcal{A} is a set of ordered pairs of vertices. The elements of \mathcal{A} are called arcs. A loop is an arc of the form (v, v) . Let $\mathcal{G} = (\mathcal{V}, \mathcal{A})$ be a directed graph with $\mathcal{V} = \{v_1, v_2, \dots, v_n\}$. A path p of length l is a sequence of vertices $v_{i_1}, v_{i_2}, \dots, v_{i_{l+1}}$ such that $(v_{i_k}, v_{i_{k+1}}) \in \mathcal{A}$ for $k = 1, 2, \dots, l$. We represent this path by $v_{i_1} \rightarrow v_{i_2} \rightarrow \dots \rightarrow v_{i_{l+1}}$ and we denote the length of the path by $|p|_1 = l$. Vertex v_{i_1} is the initial vertex of the path and $v_{i_{l+1}}$ is the final vertex of the path. The set of all paths of length l from vertex v_{i_1} to v_{i_l} is denoted by $P(v_{i_1}, v_{i_l}; l)$. When the initial and the final vertex of a path coincide, we have a circuit. An elementary circuit is a circuit in which no vertex appears more than once, except for the initial vertex, which appears exactly twice. A directed graph $\mathcal{G} = (\mathcal{V}, \mathcal{A})$ is called *strongly connected* if for any two different vertices $v_i, v_j \in \mathcal{V}$ there exists a path from v_i to v_j . If we have a directed graph $\mathcal{G} = (\mathcal{V}, \mathcal{A})$ with $\mathcal{V} = \{1, 2, \dots, n\}$ and if we associate a real number $[A]_{ij}$ with each arc $(j, i) \in \mathcal{A}$, then we say that \mathcal{G} is a weighted directed graph. We call $[A]_{ij}$ the weight of the arc (j, i) . Note that the first subscript of $[A]_{ij}$ corresponds to the final (and not the initial) vertex of the arc (j, i) .

Definition 3 (Precedence graph). Consider $A \in \mathbb{R}_{\max}^{n \times n}$. The precedence graph of A , denoted by $\mathcal{G}(A)$, is a weighted directed graph with vertices $1, 2, \dots, n$ and an arc (j, i) with weight $[A]_{ij}$ for each $[A]_{ij} \neq \varepsilon$.

Let $A \in \mathbb{R}_{\max}^{n \times n}$ and consider $\mathcal{G}(A)$. The weight $|p|_w$ of a path $p : i_1 \rightarrow i_2 \rightarrow \dots \rightarrow i_{l+1}$ is defined as the sum of the weights of the arcs that compose the path: $|p|_w = [A]_{i_2 i_1} + [A]_{i_3 i_2} + \dots + [A]_{i_{l+1} i_l} = \bigotimes_{k=1}^l [A]_{i_{k+1} i_k}$. The average weight of a circuit is defined as the weight of the circuit divided by the length of the circuit: $|p|_w / |p|_1$.

Definition 4 (Irreducibility). A matrix $A \in \mathbb{R}_{\max}^{n \times n}$ is called *irreducible* if its precedence graph is strongly connected.

Definition 5 (Max-plus eigenvalue and eigenvector). Let $A \in \mathbb{R}_{\max}^{n \times n}$. If there exist a number $\lambda \in \mathbb{R}_{\max}$ and a vector $v \in \mathbb{R}_{\max}^n$ with $v \neq \mathcal{E}_{n \times 1}$ such that $A \otimes v = \lambda \otimes v$, then we say that λ is a *max-plus eigenvalue* of A and that v is a *corresponding max-plus eigenvector* of A .

It can be shown that every square matrix with entries in \mathbb{R}_{\max} has at least one max-plus eigenvalue (see e.g. [1]). However, in contrast to linear algebra, the number of max-plus eigenvalues of an n by n matrix is in general less than n . If a matrix is irreducible, it has only one max-plus eigenvalue (see e.g. [6]).

Moreover, if v is a max-plus eigenvector of A , then $\alpha \otimes v$ with $\alpha \in \mathbb{R}$ is also a max-plus eigenvector of A . The max-plus eigenvalue has the following graph-theoretic interpretation. Consider $A \in \mathbb{R}_{\max}^{n \times n}$. If λ_{\max} is the maximal average weight over all elementary circuits of $\mathcal{G}(A)$, then λ_{\max} is a max-plus eigenvalue of A . For formulas and algorithms to determine max-plus eigenvalues and eigenvectors the interested reader is referred to [1, 4, 6, 36] and the references cited therein. Every circuit of $\mathcal{G}(A)$ with an average weight that is equal to λ_{\max} is called a critical circuit. The *critical graph* $\mathcal{G}^c(A)$ of the matrix A is the set of all critical circuits. Let \mathbb{N} be the set of positive, non-zero integers.

Theorem 6. *Let A be an irreducible matrix. Then there exists $c \in \mathbb{N}$ (the cyclicity of A), $\lambda \in \mathbb{R}$ (the unique max-plus eigenvalue of A), and $k_0 \in \mathbb{N}$ (the coupling time of A) such that*

$$\forall p \geq k_0 : A^{\otimes p+c} = \lambda^{\otimes c} \otimes A^{\otimes p} \quad (10)$$

Proof: See e.g. [1, 6, 18]. □

IV. LEGGED LOCOMOTION VIA MAX-PLUS MODELING

In Section II equations (1), (3), and (4) describe the synchronization constraints between two legs. We can generalize these equations by defining the following vectors for an n -legged robot:

$$t(k) = [t_1(k) \ \cdots \ t_n(k)]^T \quad (11)$$

$$l(k) = [l_1(k) \ \cdots \ l_n(k)]^T \quad (12)$$

Equation (1) is then written as:

$$t(k) = \tau_f \otimes l(k) \quad (13)$$

If one assumes that the synchronization is always enforced on the lift off time of a leg, equations (3) and (4) are written jointly as:

$$l(k) = \tau_g \otimes t(k-1) \oplus P \otimes t(k) \oplus Q \otimes t(k-1), \quad (14)$$

where the matrices P and Q encode the synchronization between lift off of a leg related to a touchdown of the current event (as in equation (4)) and a touchdown of the previous event (as in equation (3)), respectively. The rationale behind this particular model is to prevent that a legged platform has too many legs in swing while walking² risking falling down. Synchronization constraints are always imposed on legs that are in stance and are about to enter swing: some legs should only swing if others are in stance (equation (14)). Once in swing, legs are never constrained to go into stance (equation (13)).

²As mentioned previously in this paper we don't consider running, although it can still be achieved using the same class of models.

Equations (13) and (14) are written in state-space form as:

$$\begin{bmatrix} t(k) \\ l(k) \end{bmatrix} = \begin{bmatrix} \mathcal{E} & \tau_f \otimes E \\ P & \mathcal{E} \end{bmatrix} \otimes \begin{bmatrix} t(k) \\ l(k) \end{bmatrix} \oplus \begin{bmatrix} E & \mathcal{E} \\ \tau_g \otimes E \oplus Q & E \end{bmatrix} \otimes \begin{bmatrix} t(k-1) \\ l(k-1) \end{bmatrix} \quad (15)$$

Define the matrices

$$A_0 = \begin{bmatrix} \mathcal{E} & \tau_f \otimes E \\ P & \mathcal{E} \end{bmatrix}; \quad A_1 = \begin{bmatrix} E & \mathcal{E} \\ \tau_g \otimes E \oplus Q & E \end{bmatrix} \quad (16)$$

Consider the full state x defined as $x(k) = [t^T(k) \ l^T(k)]^T$. Equation (15) can then be written in simplified notation:

$$x(k) = A_0 \otimes x(k) \oplus A_1 \otimes x(k-1). \quad (17)$$

Note that additional max-plus identity matrices E are introduced in the diagonal of matrix A_1 . This results in the extra trivial constraints $t_i(k+1) \geq t_i(k)$ and $l_i(k+1) \geq l_i(k)$, also resulting in the final system matrix (defined in page 13, equation (35)) being irreducible. This is observed later on in Lemma 12.

A. A gait parameterization

Consider a general legged robot where a two-event circuit is associated to each leg. We present a parsimonious representation of a walking gait of a robot by grouping sets of legs and specifying in what order they are allowed to cycle.

Definition 7. Let n be the number of legs in the robot and define m as a number of leg groups. Let ℓ_1, \dots, ℓ_m be ordered sets of integers such that

$$\bigcup_{p=1}^m \ell_p = \{1, \dots, n\}, \quad \forall i \neq j, \ell_i \cap \ell_j = \emptyset, \quad \text{and} \quad \forall i, \ell_i \neq \emptyset \quad (18)$$

i.e., the sets ℓ_p form a partition of $\{1, \dots, n\}$. A gait G is defined as an ordering relation of groups of legs:

$$G = \ell_1 \prec \ell_2 \prec \dots \prec \ell_m \quad (19)$$

The gait space is the set of all gaits that satisfy the previous definitions.

By considering that each ℓ_p contains the indices of a set of legs that are synchronized in phase, the previous ordering relation is interpreted in the following manner: the set of legs indexed by ℓ_i swings synchronously. As soon as all legs in ℓ_i touchdown then all legs in ℓ_{i+1} initiate their swing motion. The same is true for ℓ_m and ℓ_1 , closing the cycle. For example, a trotting gait, where diagonal pairs of legs move synchronously, for a quadruped robot as illustrated in Figure 4, is represented by:

$$G_{\text{trot}} = \{1, 4\} \prec \{2, 3\} \quad (20)$$

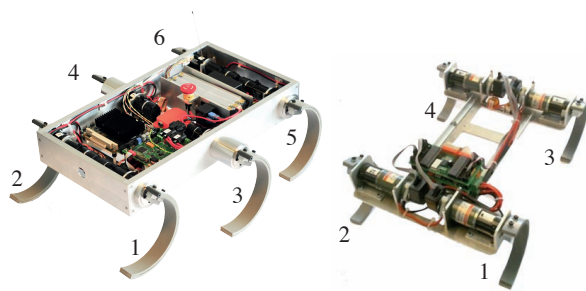


Fig. 4. Walking robots with recirculating legs inspired by RHex [47]. Zebro robot on the left and RQuad on the right both developed at DCSC, Delft University of Technology. The numbers represent the leg index numbering assumed in this paper.

The gait space defined above can represent gaits for which all legs have the same cycle time. As such, gaits where one leg cycles twice while another cycles only once are not captured by this model. Examples of such gaits are not common, but have been used on hexapod robots to transverse very inclined slopes sideways [49]. With the previous notation we can now derive the matrices P and Q in equation (15):

$$[P]_{pq} = \begin{cases} \tau_{\Delta} & \forall j \in \{1, \dots, m-1\}; \forall p \in \ell_{j+1}; \forall q \in \ell_j \\ \varepsilon & \text{otherwise} \end{cases} \quad (21)$$

$$[Q]_{pq} = \begin{cases} \tau_{\Delta} & \forall p \in \ell_1; \forall q \in \ell_m \\ \varepsilon & \text{otherwise} \end{cases} \quad (22)$$

For the trotting gait G_{trot} we obtain:

$$P_{\text{trot}} = \begin{bmatrix} \varepsilon & \varepsilon & \varepsilon & \varepsilon \\ \tau_{\Delta} & \varepsilon & \varepsilon & \tau_{\Delta} \\ \tau_{\Delta} & \varepsilon & \varepsilon & \tau_{\Delta} \\ \varepsilon & \varepsilon & \varepsilon & \varepsilon \end{bmatrix} \quad \text{and} \quad Q_{\text{trot}} = \begin{bmatrix} \varepsilon & \tau_{\Delta} & \tau_{\Delta} & \varepsilon \\ \varepsilon & \varepsilon & \varepsilon & \varepsilon \\ \varepsilon & \varepsilon & \varepsilon & \varepsilon \\ \varepsilon & \tau_{\Delta} & \tau_{\Delta} & \varepsilon \end{bmatrix} \quad (23)$$

Define the function \flat that transforms a gait into a vector of integers:

$$\flat : \{[l_1]_1, \dots, [l_1]_{i_1}\} \prec \dots \prec \{[l_m]_1, \dots, [l_m]_{i_m}\} \mapsto [[l_1]_1, \dots, [l_1]_{i_1} \dots [l_m]_1, \dots, [l_m]_{i_m}]^T \quad (24)$$

Using again the previous trotting example we get that $\flat(G_{\text{trot}}) = [1 \ 4 \ 2 \ 3]^T$ (the symbol *flat* “ \flat ” is chosen since it “flattens” the ordered collection of ordered sets of a gait into a vector). Note that the gaits $\{1, 4\} \prec \{2, 3\}$ and $\{4, 1\} \prec \{2, 3\}$ although resulting in indistinguishable motion in practice, have different mathematical representations since $\flat(\{1, 4\} \prec \{2, 3\}) \neq \flat(\{4, 1\} \prec \{2, 3\})$.

Definition 8. A gait \bar{G} is called a normal gait if the elements of the vector $\flat(\bar{G})$ are sorted increasingly.

For a gait G , define the similarity matrix $\bar{C} \in \mathbb{R}_{\max}^{n \times n}$ as:

$$[\bar{C}]_{ij} = \begin{cases} e & \text{if } [b(G)]_i = j \\ \varepsilon & \text{otherwise} \end{cases}, \forall i, j \in \{1, \dots, n\} \quad (25)$$

The similarity matrix \bar{C} is such that $\bar{C} \otimes \bar{C}^T = \bar{C}^T \otimes \bar{C} = E$. The similarity matrix associated with the trotting gait G_{trot} is:

$$\bar{C}_{\text{trot}} = \begin{bmatrix} e & \varepsilon & \varepsilon & \varepsilon \\ \varepsilon & \varepsilon & \varepsilon & e \\ \varepsilon & e & \varepsilon & \varepsilon \\ \varepsilon & \varepsilon & e & \varepsilon \end{bmatrix} = \begin{bmatrix} 0 & -\infty & -\infty & -\infty \\ -\infty & -\infty & -\infty & 0 \\ -\infty & 0 & -\infty & -\infty \\ -\infty & -\infty & 0 & -\infty \end{bmatrix} \quad (26)$$

here written in both max-plus and traditional algebra notation for legibility purposes. The similarity matrix \bar{C} has the property of “normalizing” the P and Q matrices to a max-plus algebraic lower triangular form \bar{P} and a max-plus algebraic upper triangular form \bar{Q} respectively:

$$\bar{P} = \bar{C} \otimes P \otimes \bar{C}^T \quad (27)$$

$$\bar{Q} = \bar{C} \otimes Q \otimes \bar{C}^T \quad (28)$$

Taking the previous example of the trotting gait, the normalized matrices take the form

$$\bar{P}_{\text{trot}} = \begin{bmatrix} \varepsilon & \varepsilon & \varepsilon & \varepsilon \\ \varepsilon & \varepsilon & \varepsilon & \varepsilon \\ \tau_{\Delta} & \tau_{\Delta} & \varepsilon & \varepsilon \\ \tau_{\Delta} & \tau_{\Delta} & \varepsilon & \varepsilon \end{bmatrix} \quad \text{and} \quad \bar{Q}_{\text{trot}} = \begin{bmatrix} \varepsilon & \varepsilon & \tau_{\Delta} & \tau_{\Delta} \\ \varepsilon & \varepsilon & \tau_{\Delta} & \tau_{\Delta} \\ \varepsilon & \varepsilon & \varepsilon & \varepsilon \\ \varepsilon & \varepsilon & \varepsilon & \varepsilon \end{bmatrix} \quad (29)$$

which are generated by the normal gait $\{1, 2\} \prec \{3, 4\}$. Let $\#\ell_i$ represent the number of elements of the set ℓ_i . For a general normal gait

$$\bar{G} = \ell_1 \prec \ell_2 \prec \dots \prec \ell_m \quad (30)$$

with $\bar{\mathbb{1}}_{i,j} = \mathbb{1}_{\#\ell_i \times \#\ell_j}$ the structure of the matrices \bar{P} and \bar{Q} is:

$$\bar{P} = \begin{bmatrix} \varepsilon & & \dots & \varepsilon \\ \tau_{\Delta} \otimes \bar{\mathbb{1}}_{2,1} & \varepsilon & & \vdots \\ \varepsilon & \tau_{\Delta} \otimes \bar{\mathbb{1}}_{3,2} & \varepsilon & \\ \vdots & & \ddots & \\ \varepsilon & \dots & \tau_{\Delta} \otimes \bar{\mathbb{1}}_{m,m-1} & \varepsilon \end{bmatrix}; \quad \bar{Q} = \begin{bmatrix} \varepsilon & \tau_{\Delta} \otimes \bar{\mathbb{1}}_{1,m} \\ \varepsilon & \varepsilon \end{bmatrix} \quad (31)$$

From equation (31) it is clear that the matrix \bar{P} is always max-plus nilpotent, since the upper triangle is max-plus zero. For max-plus powers of \bar{P} we obtain:

$$\bar{P}^{\otimes 2} = \begin{bmatrix} \mathcal{E} & & \cdots & & \mathcal{E} \\ \mathcal{E} & \mathcal{E} & & & \\ \tau_{\Delta} \otimes \bar{\mathbb{I}}_{3,1} & \mathcal{E} & & \mathcal{E} & \\ \vdots & \ddots & & & \vdots \\ \mathcal{E} & \cdots & \tau_{\Delta} \otimes \bar{\mathbb{I}}_{m,m-2} & \mathcal{E} & \mathcal{E} \end{bmatrix}; \quad \bar{P}^{\otimes(m-1)} = \begin{bmatrix} \mathcal{E} & \cdots & \mathcal{E} \\ \vdots & & \vdots \\ \mathcal{E} & \mathcal{E} & \\ \tau_{\Delta} \otimes \bar{\mathbb{I}}_{m,1} & \mathcal{E} & \cdots & \mathcal{E} \end{bmatrix}; \quad \bar{P}^{\otimes m} = \mathcal{E}$$

Lemma 9. *Max-plus nilpotency is invariant to max-plus similarity transformations (e.g. as defined in equations (27), (28)).*

Proof: Let \bar{P} be nilpotent and \bar{C} be a similarity matrix. Let $P = \bar{C}^T \otimes \bar{P} \otimes \bar{C}$. As such

$$P^{\otimes p} = (\bar{C}^T \otimes \bar{P} \otimes \bar{C})^{\otimes p} = \bar{C}^T \otimes \bar{P} \otimes \bar{C} \otimes \bar{C}^T \otimes \bar{P} \otimes \bar{C} \otimes \cdots \otimes \bar{C}^T \otimes \bar{P} \otimes \bar{C} = \bar{C}^T \otimes \bar{P}^{\otimes p} \otimes \bar{C} \quad (32)$$

and, $\exists p_0 > 0, \forall p \geq p_0 : P^{\otimes p} = \bar{C}^T \otimes \bar{P}^{\otimes p} \otimes \bar{C} = \mathcal{E}$. \square

Given an arbitrary gait G with associated matrices P , Q , A_0 , and A_1 one can find the normal matrix \bar{P} which is max-plus nilpotent. From Lemma 9 then P is also max-plus nilpotent. In the beginning of Section IV we have presented the synchronization equations (17) implicitly. However, if A_0^* exists then using equations (7) and (9), system (17) can be transformed into an explicit set of equations.

Lemma 10. *A sufficient condition for A_0^* to exist is that the matrix P is nilpotent in the max-plus sense.*

Proof: By direct computation, the repetitive products of A_0 can be found to be

$$A_0^{\otimes p} = \begin{cases} \left[\begin{array}{c|c} \mathcal{E} & \tau_f^{\otimes \frac{p+1}{2}} \otimes P^{\otimes \frac{p-1}{2}} \\ \hline \tau_f^{\otimes \frac{p-1}{2}} \oplus P^{\otimes \frac{p-1}{2}} & \mathcal{E} \end{array} \right] & \text{if } p \text{ is odd} \\ \left[\begin{array}{c|c} \tau_f^{\otimes \frac{p}{2}} \otimes P^{\otimes \frac{p}{2}} & \mathcal{E} \\ \hline \mathcal{E} & \tau_f^{\otimes \frac{p}{2}} \otimes P^{\otimes \frac{p}{2}} \end{array} \right] & \text{if } p \text{ is even} \end{cases} \quad (33)$$

If P is max-plus nilpotent, then there exists a finite positive integer p_0 such that $\forall p \geq p_0 : P^{\otimes p} = \mathcal{E} \Rightarrow A_0^{\otimes(2p+1)} = \mathcal{E}$, and therefore the max-plus sum for the computation of A_0^* is finite:

$$A_0^* = \bigoplus_{q=0}^{\infty} A_0^{\otimes q} = \bigoplus_{q=0}^{2p} A_0^{\otimes q} \quad (34)$$

\square

Since P is always max-plus nilpotent for gaits generated by expressions (21) and (22), we conclude that A_0^* is well defined. Let A , that we call *system matrix*, be defined by:

$$A = A_0^* \otimes A_1 \quad (35)$$

Equation (17) can be rewritten as:

$$x(k) = A_0 \otimes x(k) \oplus A_1 \otimes x(k-1) = A_0^* \otimes A_1 \otimes x(k-1) = A \otimes x(k-1). \quad (36)$$

For an arbitrary gait the internal structure of A can be quite complex. However, the gait G associated to A can be transformed into a normal gait via a similarity transformation. Let

$$C = \begin{bmatrix} \bar{C} & \mathcal{E} \\ \mathcal{E} & \bar{C} \end{bmatrix} \quad (37)$$

The similarity matrix C transforms the system matrix A of an arbitrary gait G into the system matrix \bar{A} of a normal gait \bar{G} via the similarity transformation $\bar{A} = C \otimes A \otimes C^T$. This can be shown by direct computation:

$$\begin{aligned} C \otimes A \otimes C^T &= C \otimes A_0^* \otimes C^T \otimes C \otimes A_1 \otimes C^T = \\ &= \begin{bmatrix} \bar{C} & \mathcal{E} \\ \mathcal{E} & \bar{C} \end{bmatrix} \otimes \left[\begin{array}{c|c} \mathcal{E} & \tau_f \otimes E \\ \hline P & \mathcal{E} \end{array} \right]^* \otimes \begin{bmatrix} \bar{C} & \mathcal{E} \\ \mathcal{E} & \bar{C} \end{bmatrix}^T \otimes \begin{bmatrix} \bar{C} & \mathcal{E} \\ \mathcal{E} & \bar{C} \end{bmatrix} \otimes \left[\begin{array}{c|c} E & \mathcal{E} \\ \hline \tau_g \otimes E \oplus Q & E \end{array} \right] \otimes \begin{bmatrix} \bar{C} & \mathcal{E} \\ \mathcal{E} & \bar{C} \end{bmatrix}^T = \\ &= \bigoplus_{q=0}^{2m} \left(\begin{bmatrix} \bar{C} & \mathcal{E} \\ \mathcal{E} & \bar{C} \end{bmatrix} \otimes \left[\begin{array}{c|c} \mathcal{E} & \tau_f \otimes E \\ \hline P & \mathcal{E} \end{array} \right] \otimes \begin{bmatrix} \bar{C} & \mathcal{E} \\ \mathcal{E} & \bar{C} \end{bmatrix}^T \right)^{\otimes q} \otimes \left[\begin{array}{c|c} E & \mathcal{E} \\ \hline \bar{C} \otimes (\tau_g \otimes E \oplus Q) \otimes \bar{C}^T & E \end{array} \right] = \\ &= \left(\bigoplus_{q=0}^{2m} \underbrace{\left[\begin{array}{c|c} \mathcal{E} & \tau_f \otimes E \\ \hline \bar{P} & \mathcal{E} \end{array} \right]^{\otimes q}}_{\bar{A}_0} \right) \otimes \underbrace{\left[\begin{array}{c|c} E & \mathcal{E} \\ \hline \tau_g \otimes E \oplus Q & E \end{array} \right]}_{\bar{A}_1} = \bar{A}_0^* \otimes \bar{A}_1 = \bar{A} \quad (38) \end{aligned}$$

Transforming an arbitrary gait into a normal gait is very useful since, by effectively switching rows and columns in A , one obtains a very structured matrix \bar{A} where analysis is simple. The interpretation of the similarity matrix \bar{C} is that legs can be renumbered, simplifying algebraic manipulation. Besides max-plus nilpotency, other properties are invariant to similarity transformations: irreducibility is preserved since the graphs of A and \bar{A} are equivalent up to a label renaming. Max-plus eigenvalues and eigenvectors are related by:

$$A \otimes v = \lambda \otimes v \Leftrightarrow C \otimes A \otimes C^T \otimes C \otimes v = \lambda \otimes C \otimes v \Leftrightarrow \bar{A} \otimes \bar{v} = \lambda \otimes \bar{v}, \text{ with } \bar{v} = C \otimes v \quad (39)$$

B. Structure of the system matrix \bar{A}

Let:

$$\tau_\delta = \tau_f \otimes \tau_\Delta \text{ and } \tau_\gamma = \tau_f \otimes \tau_g \quad (40)$$

The structure of \bar{A} can be obtained via a laborious but straightforward set of algebraic manipulations. For an arbitrary gait G we compute the normal gait \bar{G} via the similarity transformation with the matrix C . By observing the structures of \bar{A}_0 and \bar{A}_1 (derived from \bar{P} and \bar{Q}) a closed-form solution can be obtained for \bar{A}_0^* :

$$\bar{A}_0^* = \begin{bmatrix} W & \tau_f \otimes W \\ \bar{W} & W \end{bmatrix} \quad (41)$$

where $W = (\tau_f \otimes \bar{P})^*$, illustrated in equation (48) on page 16. The matrix \bar{W} is defined in equation (47) again on page 16. Note that $\tau_f \otimes \bar{W} \oplus E = W$ and $W \geq \bar{W}$. An expression for \bar{A} is then obtained:

$$\begin{aligned} \bar{A} &= \bar{A}_0^* \otimes \bar{A}_1 = \begin{bmatrix} W & \tau_f \otimes W \\ \bar{W} & W \end{bmatrix} \otimes \begin{bmatrix} E & \mathcal{E} \\ \tau_g \otimes E \oplus \bar{Q} & E \end{bmatrix} \\ &= \begin{bmatrix} W \oplus \tau_f \otimes \tau_g \otimes W \oplus \tau_f \otimes W \otimes \bar{Q} & \tau_f \otimes W \\ \bar{W} \oplus \tau_g \otimes W \oplus W \otimes \bar{Q} & W \end{bmatrix} \end{aligned} \quad (42)$$

Let $V = W \otimes \bar{Q}$, as illustrated by equation (49). One can show that:

$$W \otimes W = W \quad (43)$$

$$W \otimes V = V \quad (44)$$

$$V \otimes V = \tau_\delta^{\otimes(m-1)} \otimes \tau_\Delta \otimes V \quad (45)$$

Since $\mu \otimes W \geq W$ for any $\mu > 0$, and $W \geq \bar{W}$, expression (42) simplifies to:

$$\bar{A} = \begin{bmatrix} \tau_f \otimes (\tau_g \otimes W \oplus V) & \tau_f \otimes W \\ \tau_g \otimes W \oplus V & W \end{bmatrix}. \quad (46)$$

Let $t_{\ell_i}(k) = [t_{[\ell_i]_1}(k) \ t_{[\ell_i]_2}(k) \ \cdots \ t_{[\ell_i]_{\#\ell_i}}(k)]^T$ and $l_{\ell_i}(k) = [l_{[\ell_i]_1}(k) \ l_{[\ell_i]_2}(k) \ \cdots \ l_{[\ell_i]_{\#\ell_i}}(k)]^T$.

Equations (50)–(53) illustrate the resulting structure of \bar{A} written in the system form $\bar{x}(k) = \bar{A} \otimes \bar{x}(k-1)$, with $\bar{x}(k) = C \otimes x(k)$, and $\bar{E}_i = E_{\#\ell_i}$. In equation (53), the \otimes operator is omitted in unambiguous locations due to space limitations.

C. Max-plus eigenstructure of the system matrix

Given a parameterization of a gait, it is fundamental to understand whether the system $x(k) = A \otimes x(k-1)$ reaches a unique steady state behavior. In robotics this is the equivalent of asking “does the robot walk/run as specified? Is it robust to disturbances?”. These questions are answered by analyzing the max-plus eigenstructure of the system matrix: a unique eigenvalue means that the legs have a unique

$$\bar{W} = \tau_{\Delta} \otimes \begin{bmatrix} \mathcal{E} & & \cdots & \mathcal{E} \\ \bar{\mathbb{I}}_{2,1} & \mathcal{E} & & \vdots \\ \tau_{\delta} \otimes \bar{\mathbb{I}}_{3,1} & \bar{\mathbb{I}}_{3,2} & \mathcal{E} & \\ \vdots & \ddots & \ddots & \\ \tau_{\delta}^{\otimes(m-2)} \otimes \bar{\mathbb{I}}_{m,1} & \cdots & \tau_{\delta} \otimes \bar{\mathbb{I}}_{m,m-1} & \bar{\mathbb{I}}_{m,m-2} & \mathcal{E} \end{bmatrix} \quad (47)$$

$$W = \begin{bmatrix} \bar{E}_1 & & \cdots & \mathcal{E} \\ \tau_{\delta} \otimes \bar{\mathbb{I}}_{2,1} & \bar{E}_2 & & \vdots \\ \tau_{\delta}^{\otimes 2} \otimes \bar{\mathbb{I}}_{3,1} & \tau_{\delta} \otimes \bar{\mathbb{I}}_{3,2} & \bar{E}_3 & \\ \vdots & \ddots & \ddots & \\ \tau_{\delta}^{\otimes(m-1)} \otimes \bar{\mathbb{I}}_{m,1} & \cdots & \tau_{\delta}^{\otimes 2} \otimes \bar{\mathbb{I}}_{m,m-2} & \tau_{\delta} \otimes \bar{\mathbb{I}}_{m,m-1} & \bar{E}_m \end{bmatrix} \quad (48)$$

$$V = \left[\begin{array}{c|c} \mathcal{E}_{n,(n-m)} & \begin{array}{c} \tau_{\Delta} \otimes \bar{\mathbb{I}}_{1,m} \\ \tau_{\Delta} \otimes \tau_{\delta} \otimes \bar{\mathbb{I}}_{2,m} \\ \vdots \\ \tau_{\Delta} \otimes \tau_{\delta}^{\otimes(m-1)} \otimes \bar{\mathbb{I}}_{m,m} \end{array} \end{array} \right] \quad (49)$$

$$\bar{x}(k) = \bar{A} \otimes \bar{x}(k-1) \Leftrightarrow \quad (50)$$

$$\bar{x}(k) = \left[\begin{array}{c|c} \tau_{\mathbb{f}} \otimes (\tau_{\mathbb{g}} \otimes W \oplus V) & \tau_{\mathbb{f}} \otimes W \\ \hline \tau_{\mathbb{g}} \otimes W \oplus V & W \end{array} \right] \otimes \bar{x}(k-1) \Leftrightarrow \quad (51)$$

$$\begin{bmatrix} t_{\ell_1}(k) \\ \vdots \\ t_{\ell_m}(k) \\ \hline l_{\ell_1}(k) \\ \vdots \\ l_{\ell_m}(k) \end{bmatrix} = \begin{bmatrix} A_{11} & A_{12} & A_{13} \\ \hline A_{21} & A_{22} & A_{23} \\ \hline A_{31} & A_{32} & A_{33} \\ \hline A_{41} & A_{42} & A_{43} \end{bmatrix} \otimes \begin{bmatrix} t_{\ell_1}(k-1) \\ \vdots \\ t_{\ell_m}(k-1) \\ \hline l_{\ell_1}(k-1) \\ \vdots \\ l_{\ell_m}(k-1) \end{bmatrix} \Leftrightarrow \quad (52)$$

$$\underbrace{\begin{bmatrix} t_{\ell_1}(k) \\ t_{\ell_2}(k) \\ \vdots \\ t_{\ell_m}(k) \\ \hline l_{\ell_1}(k) \\ l_{\ell_2}(k) \\ \vdots \\ l_{\ell_m}(k) \end{bmatrix}}_{\bar{x}(k)} = \underbrace{\left[\begin{array}{c|c|c} \tau_{\gamma} \bar{E}_1 & \cdots & \mathcal{E} \\ \tau_{\gamma} \tau_{\delta} \bar{\mathbb{I}}_{2,1} & \tau_{\gamma} \bar{E}_2 & \vdots \\ \vdots & \ddots & \\ \hline \tau_{\gamma} \tau_{\delta}^{\otimes(m-1)} \bar{\mathbb{I}}_{m,1} & \cdots & \tau_{\gamma} \tau_{\delta} \bar{\mathbb{I}}_{m,m-1} \\ \hline \tau_{\gamma} \bar{E}_m \oplus \tau_{\delta}^{\otimes m} \bar{\mathbb{I}}_{m,m} & & \\ \hline \tau_{\mathbb{g}} \bar{E}_1 & \cdots & \mathcal{E} \\ \tau_{\mathbb{g}} \tau_{\delta} \bar{\mathbb{I}}_{2,1} & \tau_{\mathbb{g}} \bar{E}_2 & \vdots \\ \vdots & \ddots & \\ \hline \tau_{\mathbb{g}} \tau_{\delta}^{\otimes(m-1)} \bar{\mathbb{I}}_{m,1} & \cdots & \tau_{\mathbb{g}} \tau_{\delta} \bar{\mathbb{I}}_{m,m-1} \\ \hline \tau_{\mathbb{g}} \bar{E}_m \oplus \tau_{\Delta} \tau_{\delta}^{\otimes(m-1)} \bar{\mathbb{I}}_{m,m} & & \\ \hline \tau_{\delta}^{\otimes(m-1)} \bar{\mathbb{I}}_{m,1} & \cdots & \bar{E}_m \end{array} \right]}_{\bar{A}} \otimes \underbrace{\begin{bmatrix} t_{\ell_1}(k-1) \\ t_{\ell_2}(k-1) \\ \vdots \\ t_{\ell_m}(k-1) \\ \hline l_{\ell_1}(k-1) \\ l_{\ell_2}(k-1) \\ \vdots \\ l_{\ell_m}(k-1) \end{bmatrix}}_{\bar{x}(k-1)} \quad (53)$$

cycle time, and a unique (up to scaling) eigenvector means that the legs always reach the same motion pattern, independently of the initial condition or disturbances. The results obtained below use various analysis techniques available for max-plus linear systems. This is necessary due to the intrinsic time structure associated with the problem. Petri net tools (e.g. incidence matrices) can be used to understand structural properties of the system, such as irreducibility, but temporal properties are better analyzed using max-plus linear tools. In Section IV-D we show that for a fixed structure (i.e. a single Petri net) unique or non-unique eigenvectors are found by changing the holding time parameters. This result could not be captured by the Petri net structure alone. The analysis steps presented from here on are summarized in Figure 1.

Consider the following assumption (which is always satisfied in practice since the leg swing and stance times are always positive numbers):

Assumption (A1). $\tau_g, \tau_f > 0$

Lemma 11. *If assumption A1 is satisfied then*

$$\lambda := \tau_\delta^{\otimes m} \oplus \tau_\gamma \quad (54)$$

is a max-plus eigenvalue of the system matrix A (and \bar{A}) defined by equations (36) (and (50)–(53)), and $v \in \mathbb{R}_{\max}^{2n}$ defined by

$$\forall j \in \{1, \dots, m\}, \forall q \in \ell_j : \quad [v]_q := \tau_f \otimes \tau_\delta^{\otimes j-1} \quad (55)$$

$$[v]_{q+n} := \tau_\delta^{\otimes j-1} \quad (56)$$

is a max-plus eigenvector of A .

Proof: With $\bar{v} \in \mathbb{R}_{\max}^n$, let $[\bar{v}]_q = [v]_{q+n}$ for all j and $q \in \ell_j$. Then $v = [(\tau_f \otimes \bar{v})^T \quad \bar{v}^T]^T$. Recall equations (7) and (9) with new variables z and B such that $z = B \otimes z \oplus b$ with solution $z = B^* \otimes b$. Now let $z = \lambda \otimes v$, $B = A_0$, and $b = A_1 \otimes v$. We obtain

$$\lambda \otimes v = A_0 \otimes \lambda \otimes v \oplus A_1 \otimes v A_0^* \otimes A_1 \otimes v = A \otimes v \quad (57)$$

Given the previous result, it is sufficient to show that if λ and v are a max-plus eigenvalue and eigenvector of A respectively, then replacing the state variable $x(k-1)$ by v and $x(k)$ by $\lambda \otimes v$ in equation (15) holds

true:

$$\begin{aligned} \lambda \otimes v &= \lambda \otimes \begin{bmatrix} \tau_f \otimes \bar{v} \\ \bar{v} \end{bmatrix} = \lambda \otimes \left[\begin{array}{c|c} \mathcal{E} & \tau_f \otimes E \\ \hline P & \mathcal{E} \end{array} \right] \otimes v \oplus \left[\begin{array}{c|c} E & \mathcal{E} \\ \hline \tau_g \otimes E \oplus Q & E \end{array} \right] \otimes v = \\ & \left[\begin{array}{c|c} E & \lambda \otimes \tau_f \otimes E \\ \hline \lambda \otimes P \oplus \tau_g \otimes E \oplus Q & E \end{array} \right] \otimes \begin{bmatrix} \tau_f \otimes \bar{v} \\ \bar{v} \end{bmatrix} \end{aligned} \quad (58)$$

The previous expression is equivalent to the following two equations:

$$\lambda \otimes \tau_f \otimes \bar{v} = \tau_f \otimes \bar{v} \oplus \lambda \otimes \tau_f \otimes \bar{v} \quad (59)$$

$$\lambda \otimes \bar{v} = \tau_f \otimes (\lambda \otimes P \oplus \tau_g \otimes E \oplus Q) \otimes \bar{v} \oplus \bar{v} \quad (60)$$

Since $\lambda > 0$ (by assumption A1), equation (59) is always verified. Thus we focus on equation (60), which can be simplified due to $\tau_f \otimes \tau_g > 0$:

$$\lambda \otimes \bar{v} = (\tau_f \otimes \tau_g) \otimes \bar{v} \oplus \tau_f \otimes (\lambda \otimes P \oplus Q) \otimes \bar{v} \quad (61)$$

Let $\tau_\Delta \otimes P_0 = P$ and $\tau_\Delta \otimes Q_0 = Q$, i.e., all entries of matrices P_0 and Q_0 are either e or ε to obtain (recall that $\tau_\delta = \tau_f \otimes \tau_\Delta$ and $\tau_\gamma = \tau_f \otimes \tau_g$):

$$\lambda \otimes \bar{v} = \tau_\gamma \otimes \bar{v} \oplus \tau_\delta \otimes (\lambda \otimes P_0 \oplus Q_0) \otimes \bar{v} \quad (62)$$

We now consider two cases:

i) First we analyze the row indices of equation (62) that are elements of the sets ℓ_2, \dots, ℓ_m . For each $j \in \{1, \dots, m-1\}$ and for each row $p \in \ell_{j+1}$ we obtain (notice that according to (22) all the elements of $[Q_0]_{p,\cdot}$ are ε since $p \notin \ell_1$, and that $[\bar{v}]_p = \tau_\delta^{\otimes j}$ for $p \in \ell_{j+1}$):

$$[\lambda \otimes \bar{v}]_p = [\tau_\gamma \otimes \bar{v}]_p \oplus \tau_\delta \otimes [\lambda \otimes P_0 \oplus Q_0 \otimes \bar{v}]_p \Leftrightarrow \quad (63)$$

$$\lambda \otimes [\bar{v}]_p = \tau_\gamma \otimes [\bar{v}]_p \oplus \tau_\delta \otimes [\lambda \otimes P_0]_{p,\cdot} \otimes \bar{v} \oplus \underbrace{[Q_0]_{p,\cdot}}_{\varepsilon} \otimes \bar{v} \Leftrightarrow \quad (64)$$

$$\lambda \otimes \tau_\delta^{\otimes j} = \tau_\gamma \otimes \tau_\delta^{\otimes j} \oplus \tau_\delta \otimes \bigoplus_{q \in \ell_j} \lambda \otimes \underbrace{[P_0]_{p,q}}_e \otimes [\bar{v}]_q \Leftrightarrow \quad (65)$$

$$\lambda \otimes \tau_\delta^{\otimes j} = \tau_\gamma \otimes \tau_\delta^{\otimes j} \oplus \tau_\delta \otimes \lambda \otimes \tau_\delta^{\otimes j-1} \Leftrightarrow \quad (66)$$

$$\lambda \otimes \tau_\delta^{\otimes j} = \tau_\gamma \otimes \tau_\delta^{\otimes j} \oplus \lambda \otimes \tau_\delta^{\otimes j} \quad (67)$$

The last term always holds true since $\lambda \geq \tau_\gamma$. Thus for rows $p \in \ell_2, \dots, \ell_m$ equation (62) holds true.

ii) We now look at all the remaining rows p such that $p \in \ell_1$ (noticing now that according to (21) all the

elements of $[P_0]_{p,\cdot}$ are ε and that $[\bar{v}]_p = e$ since $p \in \ell_1$):

$$[\lambda \otimes \bar{v}]_p = [\tau_\gamma \otimes \bar{v}]_p \oplus \tau_\delta \otimes [\lambda \otimes P_0 \oplus Q_0]_{p,\cdot} \otimes \bar{v} \Leftrightarrow \quad (68)$$

$$\lambda \otimes [\bar{v}]_p = \tau_\gamma \oplus \tau_\delta \otimes \underbrace{[\lambda \otimes P_0]_{p,\cdot}}_{\varepsilon} \otimes \bar{v} \oplus \tau_\delta \otimes [Q_0]_{p,\cdot} \otimes \bar{v} \Leftrightarrow \quad (69)$$

$$\lambda = \tau_\gamma \oplus \tau_\delta \otimes \bigoplus_{q \in \ell_m} \underbrace{[Q_0]_{p,q}}_e \otimes [\bar{v}]_q \Leftrightarrow \quad (70)$$

$$\lambda = \tau_\gamma \oplus \tau_\delta \otimes \tau_\delta^{\otimes m-1} \Leftrightarrow \quad (71)$$

$$\lambda = \tau_\gamma \oplus \tau_\delta^{\otimes m} \quad (72)$$

Combining i) and ii) we conclude that equation (62) holds true. \square

Consider again the trotting gait for a quadruped G_{trot} defined in (20). For this gait $m = 2$, resulting in:

$$v_{\text{trot}} = \left[\tau_f \quad (\tau_\Delta \otimes \tau_f^{\otimes 2}) \quad (\tau_\Delta \otimes \tau_f^{\otimes 2}) \quad \tau_f \quad 0 \quad (\tau_\Delta \otimes \tau_f) \quad (\tau_\Delta \otimes \tau_f) \quad 0 \right]^T; \quad \lambda_{\text{trot}} = (\tau_f \otimes \tau_\Delta)^{\otimes 2} \oplus \tau_f \otimes \tau_g$$

Lemma 12. *Matrices A and \bar{A} are irreducible.*

Proof: The sub-matrices $A_{12}, A_{22}, A_{32}, A_{42}, A_{21}$ defined in expressions (52) and (53) have all their elements different from ε . The sub-matrix A_{23} has all diagonal elements different from ε . As such, any node can be reached by any other node via the rows defined by $A_{12}, A_{22}, A_{32}, A_{42}$ and the columns defined by A_{21}, A_{22}, A_{23} . Therefore \bar{A} is irreducible. Since A is a similarity transformation away from \bar{A} then we conclude that A is also irreducible. \square

Corollary 13. *The max-plus eigenvalue λ of A (and \bar{A}) given by (54) is unique.*

The max-plus eigenvector v defined by (55)–(56) is not necessarily unique, given assumption A1 alone. Since, to the authors' best knowledge, there exists no algebraic method to prove max-plus eigenvector uniqueness in general, we take advantage of the precedence graph of \bar{A} to further investigate this property. If the critical graph of an irreducible max-plus system matrix has a single strongly connected subgraph, then its max-plus eigenvector is unique up to a max-plus scaling factor (see [1], Theorem 3.101). We proceed by computing the critical graph(s) of \bar{A} .

D. The precedence graph of \bar{A}

Given expression (53) it is possible to construct the precedence graph of \bar{A} . Since this graph can be quite large for a general \bar{A} , we find it more efficient to first group “similar” nodes into a single node, i.e. apply a procedure called node reduction (Figure 5). Next, we show various subgraphs of the graph of \bar{A} to better illustrate its structure (Figure 6). The total precedence graph of \bar{A} is thus the combination

of Figures 5 and 6. The process of constructing the graph of \bar{A} starts by grouping all nodes of an event associated with a group of legs ℓ_i into a single node. This can be accomplished since event nodes from the same group of legs ℓ_i have “similar” incoming and outgoing arcs. As an example, consider the first set of $\#\ell_1$ rows of \bar{A} as defined in expression (53):

$$t_{\ell_1}(k) = \tau_\gamma \otimes E_1 \otimes t_{\ell_1}(k-1) \oplus \tau_\delta \otimes \mathbb{1}_{1,m} \otimes t_{\ell_m}(k-1) \oplus \tau_f \otimes E_1 \otimes l_{\ell_1}(k-1) \quad (73)$$

The precedence graph for equation (73) consists of $3 \times \#\ell_1$ nodes, since it involves the vectors t_{ℓ_1} , t_{ℓ_m} , and l_{ℓ_1} . The relation between $t_{\ell_1}(k)$ and $t_{\ell_1}(k-1)$ results in $\#\ell_1$ self connected arcs in the t_{ℓ_1} events with weights τ_γ . Instead of expressing all elements of t_{ℓ_1} as individual nodes with self arcs, we reduce then to a single node with one self arc, as seen in Figure 5-a2. The dashed attribute used on the self arc indicates that for each node in the group only self arcs exist, as expressed by the “connecting” matrix E_1 . The relation between $t_{\ell_1}(k)$ and $t_{\ell_m}(k-1)$ is somewhat more involved, since it contains $\#\ell_1 \times \#\ell_m$ arcs, as expressed by the connecting matrix $\mathbb{1}_{1,m}$. The resulting node reduction is illustrated in Figure 5-b1. The node reduction for the relation between t_{ℓ_1} and l_{ℓ_1} is illustrated in Figure 5-a4. Again we use dashed attributes on the arcs to represent the connecting matrix E_1 . For all other relations with connecting matrices $\mathbb{1}$ we use solid arcs. We make an exception in Figures 5-c1 to 5-c4 where different line attributes are used to distinguish arcs from $t_{\ell_p} \rightarrow t_{\ell_q}$, $t_{\ell_p} \rightarrow l_{\ell_q}$, etc. The same line attributes are used in Figures 6-c1 and 6-c2. Note that multiple incoming arcs to a node are related via the \oplus operation, e.g. as in the example (73) the node t_{ℓ_1} has 3 incoming arcs, illustrated in Figure 6. The following list summarizes the node reduction:

- Figure 5-a1 illustrates node reduction of the term $\tau_\delta^{\otimes m} \otimes \mathbb{1}_{m,m}$ of sub-matrix A_{22} from expressions (52) and (53)
- Figure 5-a2 illustrates the node reduction of the block diagonal of matrix A_{11} and the $\tau_\gamma \otimes \bar{E}_m$ term of A_{22} .
- Figure 5-a3 illustrates the node reduction of the block diagonal of matrix $[A_{33}^T \ A_{43}^T]^T$
- Figure 5-a4 illustrates the node reduction of the term $\tau_g \otimes E_m$ of sub-matrix A_{42} together with the block diagonals of matrices A_{31} and $[A_{13}^T \ A_{23}^T]^T$
- Figures 5-b1 and 5-b2 illustrate the node reduction for the columns formed by the matrices (not including the term $\tau_g \otimes E_m$ from matrix A_{42} already represented in Figure 5-a4) A_{12} and $[A_{32}^T \ A_{42}^T]^T$ respectively
- Figures 5-c1 to 5-c4 illustrate the node reduction of the off-diagonal elements of matrices $\tau_\gamma \otimes W$, $\tau_f \otimes W$, $\tau_g \otimes W$, and W , from expression (51) respectively.

Given the node reduction one can now proceed to construct the precedence graph of \bar{A} :

- Figure 6-a is the graph of the block diagonal of \bar{A} together with the block diagonals of the submatrices $\begin{bmatrix} A_{31} & A_{32} \\ A_{41} & A_{42} \end{bmatrix}$ and $[A_{13}^T \quad A_{23}^T]^T$ using the node reductions presented in Figures 5-a1 to 5-a4.
- Figure 6-b is the graph of the columns formed by the matrices A_{12} and $[A_{32}^T \quad A_{42}^T]^T$ using node reductions presented in Figures 5-b1 and 5-b2.
- Figures 6-c1 and 6-c2 illustrate two subgraphs of the remaining columns of \bar{A} . Note that we only present the subgraphs of the first sets of $\#\ell_1$ and $\#\ell_2$ out of a total of $m - 1$ columns. These follow the same pattern. We use different attributes on the arcs, such as dashed, thick solid, etc., to distinguish the different node reductions, as presented in Figures 5-c1 to 5-c4.

Consider the following assumption:

Assumption (A2). $\tau_\gamma \leq \tau_\delta^{\otimes m}$

Lemma 14. *If assumption A2 is verified then the critical graph of $\mathcal{G}^c(A)$ (and $\mathcal{G}^c(\bar{A})$) has a single strongly connected subgraph.*

Proof: We consider two cases:

i) $\tau_\gamma = \tau_\delta^{\otimes m} = \lambda$.

In this situation the circuits presented in Figures 5-a1 and 5-a2 all belong to the critical graph since their weights are τ_γ or $\tau_\delta^{\otimes m}$ both equal to the max-plus eigenvalue λ . Note that any circuit c_1 of length l made from the nodes of t_{ℓ_m} , illustrated in Figure 5-a1, has an average weight of

$$\frac{|c_1|_w}{|c_1|_1} = \frac{(\tau_\delta^{\otimes m})^{\otimes l}}{l} = \tau_\delta^{\otimes m} = \lambda \quad (74)$$

and as such also belongs to the critical graph. Any other circuit in the precedence graph of \bar{A} must pass through at least one node of t_{ℓ_m} , as illustrated in Figures 6-b, 6-c1, and 6-c2 (with the exception of the self-loops in Figure 5-a3 and the circuits in Figure 5-a4 that we don't consider since their weights are e and $\tau_\gamma/2$ both less than λ). Additionally, arcs starting in nodes from a group t_{ℓ_q} with $q < m$ are only connected to nodes in $t_{\ell_{q+p}}$ for $p \geq 0$ (or $l_{\ell_{q+p}}$). This is again illustrated in Figures 6-a, 6-c1, and 6-c2. Let $t_{[\ell_q]_i}$ denote element i of t_{ℓ_q} . Consider the circuit

$$c_2 : t_{[\ell_m]_i} \rightarrow t_{[\ell_q]_j} \rightarrow t_{[\ell_m]_i} \quad (75)$$

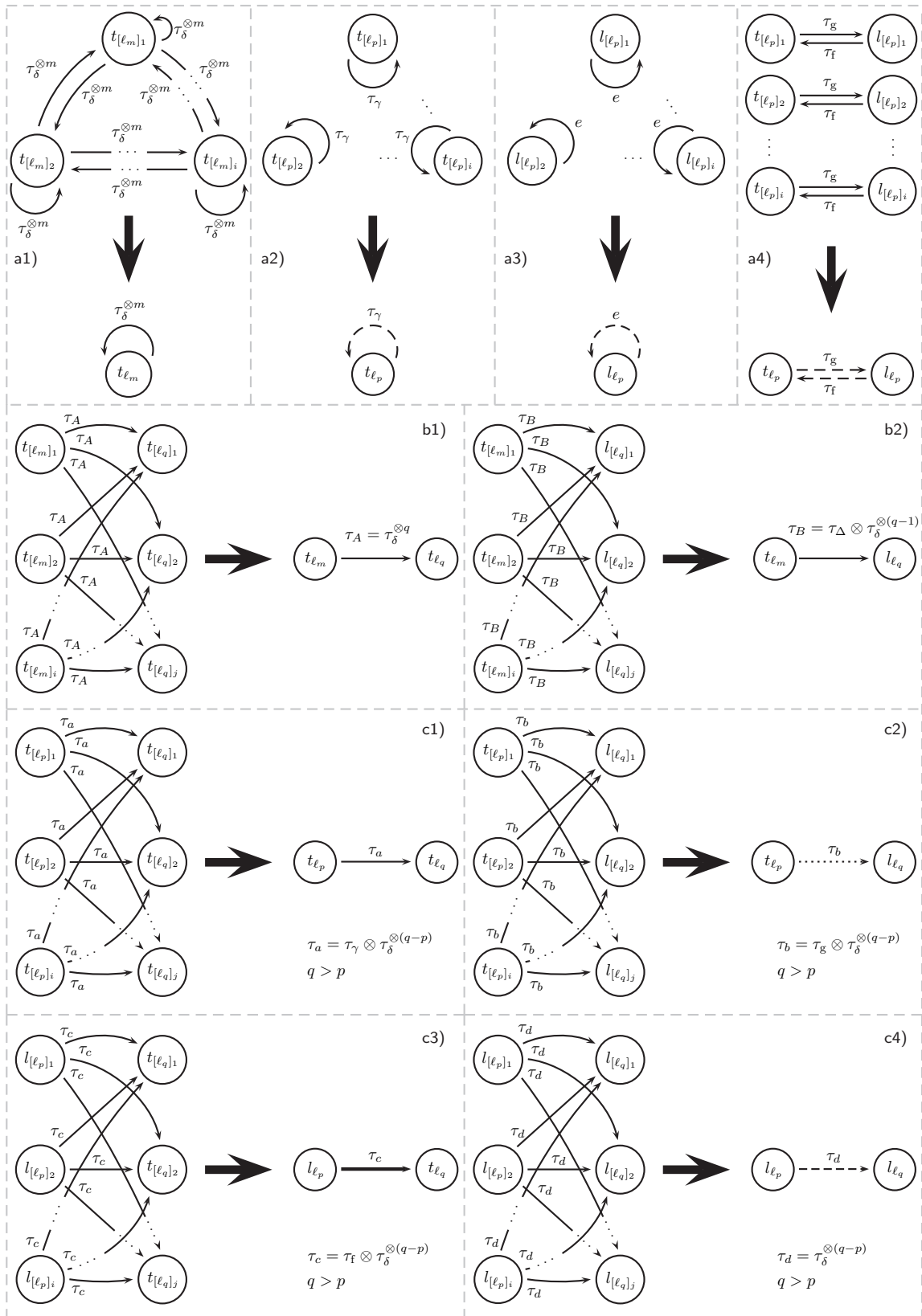


Fig. 5. Graph reductions. Touchdown and lift off events with indexes belonging to the same set ℓ_q can be grouped together since they have the same number of output and input arcs with the same weights.

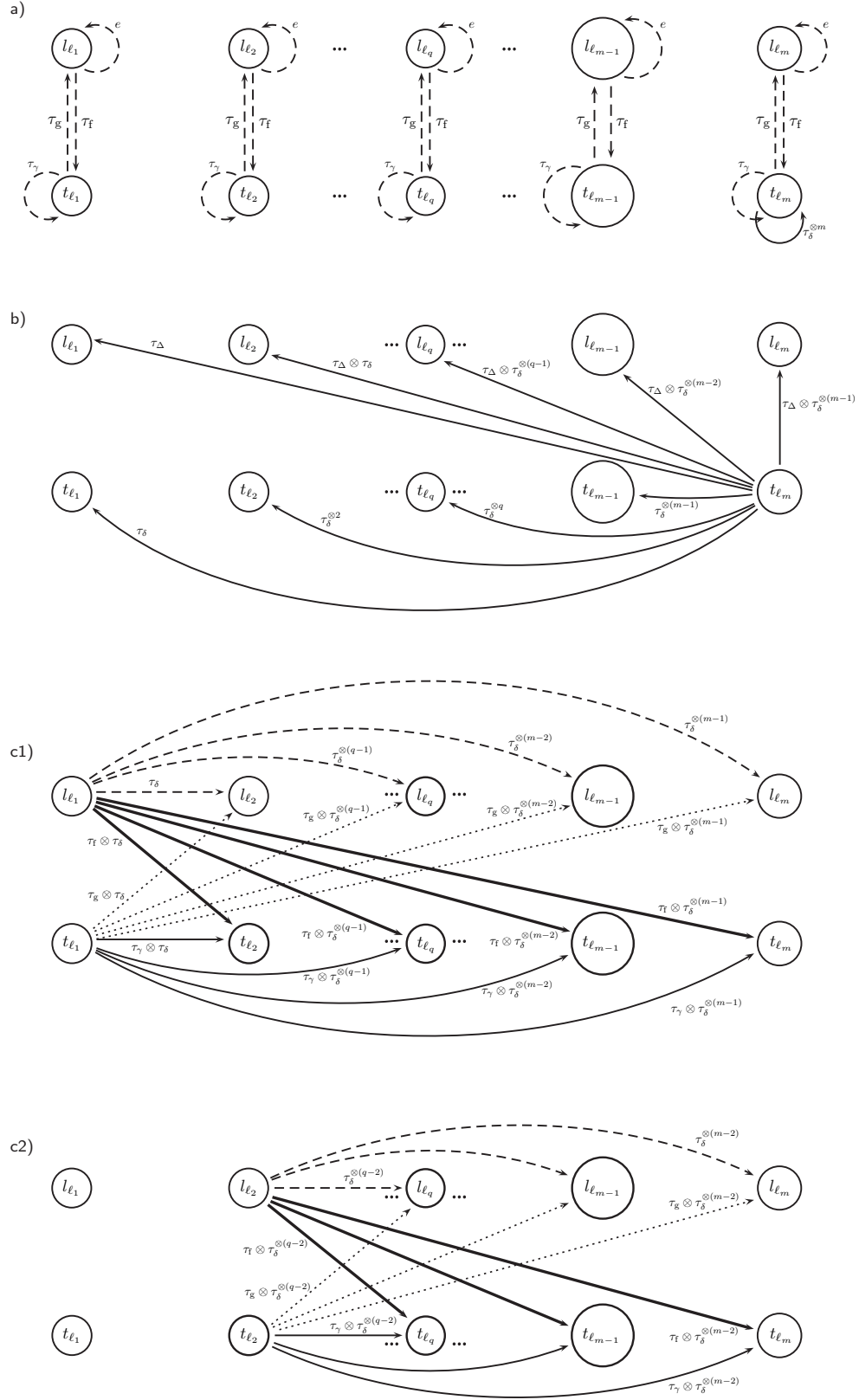


Fig. 6. Elements of the precedence graph of the system matrix A . The total precedence graph of A is composed of all the arcs presented in a) and b), together with the $m - 1$ remaining subgraphs that follow the pattern of Figures c1) and c2).

with $q < m$. The average weight is (with $\tau_\gamma = \tau_\delta^{\otimes m}$)

$$\frac{|c_2|_w}{|c_2|_1} = \frac{\tau_\delta^{\otimes q} \otimes \tau_\gamma \otimes \tau_\delta^{\otimes (m-q)}}{2} = \frac{\tau_\delta^{\otimes m} \otimes \tau_\gamma}{2} = \lambda \quad (76)$$

Circuit c_2 is thus also in the critical graph. For the general circuit of the type

$$c_3 : t_{[\ell_m]_i} \rightarrow \underbrace{t_{[\ell_{q_1}]_{j_1}} \rightarrow t_{[\ell_{q_2}]_{j_2}} \rightarrow \cdots \rightarrow t_{[\ell_{q_l}]_{j_l}}}_{l \text{ nodes}} \rightarrow t_{[\ell_m]_i} \quad (77)$$

with $q_1 < q_2 < \cdots < q_l < m$, the average weight is

$$\frac{|c_3|_w}{|c_3|_1} = \frac{\tau_\gamma^{\otimes l} \otimes \tau_\delta^{\otimes q_1} \otimes \tau_\delta^{\otimes (q_2 - q_1)} \otimes \cdots \otimes \tau_\delta^{\otimes (m - q_l)}}{l + 1} = \frac{\tau_\gamma^{\otimes l} \otimes \tau_\delta^{\otimes m}}{l + 1} = \lambda. \quad (78)$$

Again, circuit c_3 is part of the critical graph. Any circuit that passes through any node in l_{ℓ_q} , for any q , will never be in the critical graph. This is due to the fact that arcs within touchdown nodes of different leg groups yield a higher weight:

$$t_{[\ell_q]_i} \rightarrow t_{[\ell_p]_j} \quad \text{weight: } \tau_\gamma \otimes \tau_\Delta^{\otimes (q-p)} \quad (79)$$

$$t_{[\ell_q]_i} \rightarrow l_{[\ell_p]_j} \quad \text{weight: } \tau_g \otimes \tau_\Delta^{\otimes (q-p)} \quad (80)$$

$$l_{[\ell_q]_i} \rightarrow t_{[\ell_p]_j} \quad \text{weight: } \tau_f \otimes \tau_\Delta^{\otimes (q-p)} \quad (81)$$

$$l_{[\ell_q]_i} \rightarrow l_{[\ell_p]_j} \quad \text{weight: } \tau_\Delta^{\otimes (q-p)} \quad (82)$$

As such, a path that connects a touchdown node to a lift off node ‘loses’ $\tau_\gamma - \tau_g = \tau_f$ from the maximum possible weight, a path from lift off to lift off nodes loses τ_γ , and a path from lift off nodes to touchdown nodes loses τ_g in weight. This can also be observed in the structure of \bar{A} , in equation (51), where the sub-matrix $\tau_f \otimes (\tau_g \otimes W \oplus V)$ overcomes the sub-matrices $\tau_g \otimes W \oplus V$, $\tau_f \otimes W$, and W . Consider, for example, the circuit c_4 :

$$c_4 : t_{[\ell_m]_i} \rightarrow t_{[\ell_p]_{j_0}} \rightarrow l_{[\ell_{p+q}]_{j_q}} \rightarrow t_{[\ell_m]_i} \quad (83)$$

then

$$\frac{|c_4|_w}{|c_4|_1} = \frac{\tau_\delta^{\otimes p} \otimes (\tau_g \otimes \tau_\delta^{\otimes q}) \otimes (\tau_f \otimes \tau_\delta^{\otimes (m-(p+q))})}{3} = \frac{\tau_\gamma \otimes \tau_\delta^{\otimes m}}{3} < \lambda. \quad (84)$$

Since all the nodes in the critical graph are connected (they are all touchdown nodes) we conclude that for the case $\tau_\gamma = \tau_\delta^{\otimes m} = \lambda$ the critical graph of \bar{A} has a single strongly connected subgraph. Figure 7-a illustrates the complete critical graph of \bar{A} for this case.

ii) $\tau_\gamma < \tau_\delta^{\otimes m} = \lambda$.

In this situation only circuits of the type c_1 are part of the critical graph. Circuits of the type c_2 or c_3 are not part of the critical graph. Figure 7-b illustrates the resulting critical graph of \bar{A} . Since all the nodes

of t_{ℓ_m} are connected to each other we conclude that for the case $\tau_\gamma < \tau_\delta^{\otimes m} = \lambda$ the critical graph of \bar{A} has a single strongly connected subgraph.

A third case can be considered: $\tau_\delta^{\otimes m} < \tau_\gamma = \lambda$. In this situation the critical graph of \bar{A} does not have a single strongly connected subgraph. Figure 7-c illustrates this situation, that we document here without proof. \square

Theorem 15. *Given assumptions A1 and A2, the max-plus eigenvalue λ of the system matrix A (and \bar{A}), defined by equation (54), is unique, and the max-plus eigenvector v of A (and \bar{A}), defined by equations (55)–(56) is unique up to a max-plus scaling factor.*

Proof: According to Lemma 12 A is irreducible, and as such it has a unique max-plus eigenvalue. According to Lemma 14 the critical graph of $\mathcal{G}^c(A)$ has a single strongly connected subgraph, and as such its max-plus eigenvector is unique up to a max-plus scaling factor (see [1], Theorem 3.101). \square

E. Coupling time

Theorem 6 on page 9 describes an important property of max-plus-linear systems when the system matrix A is irreducible: it guarantees the existence of an autonomous steady-state regime that is achieved in a number of finite steps k_0 , called the *coupling time*. Computing the coupling time is very important for the application of legged locomotion since it provides the number of steps a robot needs to take to reach steady state after a gait transition or a perturbation.

Lemma 16. *Given assumptions A1, A2, the coupling time for the max-plus-linear system defined by equation (15) is $k_0 = 2$ with cyclicity $c = 1$.*

Proof: Computing successive products of \bar{A} and taking advantage of its structure and equations (43)–(45) one can write its p -th power $\bar{A}^{\otimes p}$, valid for all $p \geq 2$, illustrated by equations (88) and (90). By inspection of the expression of $\bar{A}^{\otimes p}$ in (88)–(90) one can observe that most terms are max-plus multiplying by a power of the max-plus eigenvalue λ (recall that with assumption A2 we have $\lambda = \tau_\delta^{\otimes m}$). To factor out λ of the matrix composed by expressions (88) and (90) we show that

$$\begin{aligned} \lambda^{\otimes(p-2)} \otimes \tau_f \otimes \tau_g \otimes V \otimes W &\geq \tau_f^{\otimes(p-1)} \otimes \tau_g^{\otimes p} \otimes W \Leftrightarrow \\ \tau_g \otimes \lambda^{\otimes(p-2)} \otimes \tau_f \otimes V \otimes W &\geq \tau_g \otimes \tau_\gamma^{\otimes(p-1)} \otimes W \end{aligned} \quad (85)$$

Since $\lambda \geq \tau_\gamma$ it is sufficient to show that

$$\tau_f \otimes V \otimes W \geq \tau_\gamma \otimes W \quad (86)$$

This can be confirmed by inspecting equations (48) and (92):

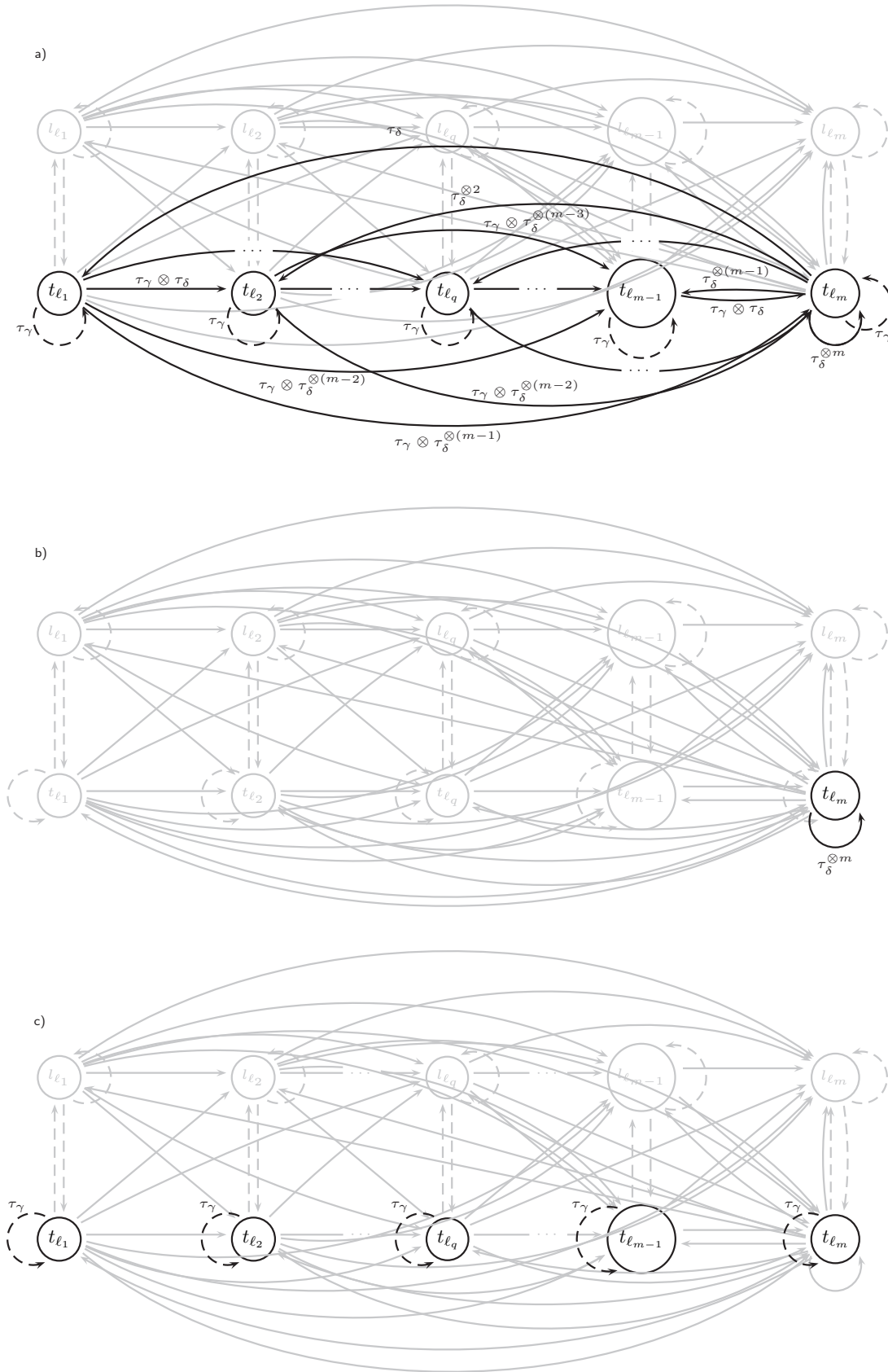


Fig. 7. Critical graphs of the system matrix \bar{A} . a) Case 1: $\tau_\gamma = \tau_\delta^{\otimes m} = \lambda$. b) Case 2: $\tau_\gamma < \tau_\delta^{\otimes m} = \lambda$. c) Case 3: $\tau_\delta^{\otimes m} < \tau_\gamma = \lambda$.

$$[\bar{A}^{\otimes p}]_{.,1} = \begin{bmatrix} \tau_f \otimes \left(\lambda^{\otimes(p-2)} \otimes \tau_f \otimes \tau_g \otimes V \otimes W \oplus \lambda^{\otimes(p-1)} \otimes V \oplus \tau_f^{\otimes(p-1)} \otimes \tau_g^{\otimes p} \otimes W \right) \\ \lambda^{\otimes(p-2)} \otimes \tau_f \otimes \tau_g \otimes V \otimes W \oplus \lambda^{\otimes(p-1)} \otimes V \oplus \tau_f^{\otimes(p-1)} \otimes \tau_g^{\otimes p} \otimes W \end{bmatrix} \quad (88)$$

$$= \begin{bmatrix} \tau_f \otimes \left(\lambda^{\otimes(p-2)} \otimes \tau_f \otimes \tau_g \otimes V \otimes W \oplus \lambda^{\otimes(p-1)} \otimes V \right) \\ \lambda^{\otimes(p-2)} \otimes \tau_f \otimes \tau_g \otimes V \otimes W \oplus \lambda^{\otimes(p-1)} \otimes V \end{bmatrix} \quad (89)$$

$$[\bar{A}^{\otimes p}]_{.,2} = \begin{bmatrix} \tau_f \otimes \left(\lambda^{\otimes(p-2)} \otimes \tau_f \otimes V \otimes W \oplus (\tau_f \otimes \tau_g)^{\otimes(p-1)} \otimes W \right) \\ \lambda^{\otimes(p-2)} \otimes \tau_f \otimes V \otimes W \oplus (\tau_f \otimes \tau_g)^{\otimes(p-1)} \otimes W \end{bmatrix} \quad (90)$$

$$= \begin{bmatrix} \tau_f \otimes \left(\lambda^{\otimes(p-2)} \otimes \tau_f \otimes V \otimes W \right) \\ \lambda^{\otimes(p-2)} \otimes \tau_f \otimes V \otimes W \end{bmatrix} \quad (91)$$

$$\tau_f \otimes V \otimes W = \begin{bmatrix} \tau_\delta^{\otimes m} \otimes \bar{\mathbb{1}}_{1,1} & \cdots & \tau_\delta \otimes \bar{\mathbb{1}}_{1,m} \\ \vdots & \ddots & \vdots \\ \tau_\delta^{\otimes(2m-1)} \otimes \bar{\mathbb{1}}_{m,1} & \cdots & \tau_\delta^{\otimes m} \otimes \bar{\mathbb{1}}_{m,m} \end{bmatrix} \quad (92)$$

$$\bar{A}^{\otimes(p+1)} = \begin{bmatrix} \tau_f \otimes \left(\lambda^{\otimes(p-1)} \otimes \tau_f \otimes \tau_g \otimes V \otimes W \oplus \lambda^{\otimes p} \otimes V \right) & \tau_f \otimes \left(\lambda^{\otimes(p-1)} \otimes \tau_f \otimes V \otimes W \right) \\ \lambda^{\otimes(p-1)} \otimes \tau_f \otimes \tau_g \otimes V \otimes W \oplus \lambda^{\otimes p} \otimes V & \lambda^{\otimes(p-1)} \otimes \tau_f \otimes V \otimes W \end{bmatrix} \quad (93)$$

$$= \lambda \otimes \begin{bmatrix} \tau_f \otimes \left(\lambda^{\otimes(p-2)} \otimes \tau_f \otimes \tau_g \otimes V \otimes W \oplus \lambda^{\otimes(p-1)} \otimes V \right) & \tau_f \otimes \left(\lambda^{\otimes(p-2)} \otimes \tau_f \otimes V \otimes W \right) \\ \lambda^{\otimes(p-2)} \otimes \tau_f \otimes \tau_g \otimes V \otimes W \oplus \lambda^{\otimes(p-1)} \otimes V & \lambda^{\otimes(p-2)} \otimes \tau_f \otimes V \otimes W \end{bmatrix} \quad (94)$$

$$= \lambda \otimes \bar{A}^{\otimes p} \quad (95)$$

- 1) All the terms in the upper block triangle of $\tau_\gamma \otimes W$ are ε while for $\tau_f \otimes V \otimes W$ they are positive numbers.
- 2) In the block diagonal $[\tau_f \otimes V \otimes W]_{i,i} = \tau_\delta^{\otimes m} \otimes \mathbb{1} \geq \tau_\gamma \otimes E = [\tau_\gamma \otimes W]_{i,i}$, by assumption A2.
- 3) In the lower block triangle $[\tau_f \otimes V \otimes W]_{i,j} = \tau_\delta^{\otimes(m+i-j)} \otimes \mathbb{1} \geq \tau_\delta^{\otimes(i-j)} \otimes \tau_\gamma \otimes \mathbb{1} = [\tau_\gamma \otimes W]_{i,j}$, by assumption A2.

Taking advantage of this simplification one can obtain equations (89), (91), and (93)–(95). Together with the similarity transformation we obtain the result valid for $p \geq 2$:

$$A^{\otimes(p+1)} = C \otimes \bar{A}^{\otimes(p+1)} \otimes C^T = C \otimes \lambda \otimes \bar{A}^{\otimes p} \otimes C^T = \lambda \otimes A^{\otimes p}, \quad (87)$$

thus concluding that the coupling time is $k_0 = 2$ with cyclicity $c = 1$. \square

V. CONCLUSIONS

We have shown that max-plus linear models are very well suited to model leg synchronization in legged locomotion. The abstraction of the continuous-time dynamics associated with each leg as a two-event circuit simplifies the construction of a gait space. The combinatorial nature of this gait space, arising

from all the possible arrangements in which multiple legs can be synchronized, is captured by a compact representation as an ordered set of ordered sets.

For the classes of switching max-plus linear systems developed in this paper important structural properties of the max-plus system matrix are obtained in closed-form. The unique max-plus eigenvalue represents the total cycle time, the unique (up to a scaling factor) max-plus eigenvector dictates a unique steady-state behavior, and the coupling time reveals the transient response to gait switching or disturbances.

Although some of the derivations in this paper are quite lengthy, using a combination of discrete-event algebraic tools with graph-theoretic concepts has led to an important result in robotics: since the coupling time was found to be two, we have shown that legged robots can switch gaits (or rhythms) or recover from large disturbances in at least two steps. In the derivation process we have found that similarity transformations can facilitate the algebraic manipulations by exposing the structure of the system matrices. This was important to find closed-form expressions to the eigen-structure of the system and the coupling time, that typically need to be computed via simulations or using numerical procedures. On the graph side, the node-reduction procedure has allowed depicting graphs that can have an arbitrary large number of nodes. A graph-theoretic proof is needed for proving the uniqueness of the max-plus eigenvector. Our results are valid for robots with an arbitrary number of legs.

Further research will look towards relaxing the structure of the system matrix to address the synchronization of general cyclic systems and towards the modeling of more general gaits.

REFERENCES

- [1] F. Baccelli, G. Cohen, G. Olsder, and J. Quadrat. *Synchronization and Linearity: an Algebra for Discrete Event Systems*. Wiley, 1992.
- [2] B. Bede and H. Nobuhara. A novel max-plus algebra based wavelet transform and its applications in image processing. In *Proc. of the IEEE Int. Conf. on Systems, Man and Cybernetics*, pages 2585–2588, San Antonio, Texas, USA, 2009.
- [3] J.G. Braker. Max-algebra modelling and analysis of time-table dependent transportation networks. In *Proc. of the First European Control Conf.*, pages 1831–1836, Grenoble, France, 1991.
- [4] J.G. Braker and G.J. Olsder. The power algorithm in max algebra. *Linear Algebra and Its Applications*, 182:67–89, 1993.
- [5] A. Cohen, S. Rossignol, and S. Grillner. *Neural Control of Rhythmic Movements in Vertebrates*. Wiley, 1988.
- [6] G. Cohen, D. Dubois, J. Quadrat, and M. Viot. A linear-system-theoretic view of discrete-event processes and its use for performance evaluation in manufacturing. *IEEE Tran. on Automatic Control*, 30(3):210–220, 1985.

- [7] G. Cohen, D. Dubois, J.P. Quadrat, and M. Viot. A linear-system-theoretic view of discrete-event processes. In *Proc. of the 22nd IEEE Conf. on Decision and Control*, pages 1039–1044, San Antonio, Texas, December 1983.
- [8] G. Cohen, P. Moller, J.P. Quadrat, and M. Viot. Algebraic tools for the performance evaluation of discrete event systems. *Proc. of the IEEE*, 77(1):39–58, January 1989.
- [9] R.A. Cuninghame-Green. Process synchronisation in a steelworks – A problem of feasibility. In J. Banbury and J. Maitland, editors, *Proc. of the 2nd Int. Conf. on Operational Research*, pages 323–328, Aix-en-Provence, France, 1961. London: English Universities Press.
- [10] R.A. Cuninghame-Green. Describing industrial processes with interference and approximating their steady-state behaviour. *Operational Research Quarterly*, 13(1):95–100, 1962.
- [11] R.A. Cuninghame-Green. *Minimax Algebra*, volume 166 of *Lecture Notes in Economics and Mathematical Systems*. Springer-Verlag, 1979.
- [12] B. De Schutter and T. van den Boom. Max-plus algebra and max-plus linear discrete event systems: An introduction. In *Proc. of the 9th Int. Workshop on Discrete Event Systems*, pages 36–42, Göteborg, Sweden, May 2008.
- [13] F. Dorfler and F. Bullo. Exploring synchronization in complex oscillator networks. In *IEEE Conf. on Decision and Control*, Maui, HI, USA, December 2012. To appear.
- [14] R. Full and D.E. Koditschek. Templates and anchors: neuromechanical hypotheses of legged locomotion on land. *J. of Experimental Biology*, 202(23):3325–3332, 1999.
- [15] S. Gaubert. An algebraic method for optimizing resources in timed event graphs. In A. Bensoussan and J.L. Lions, editors, *Proc. of the 9th Int. Conf. on Analysis and Optimization of Systems*, volume 144 of *Lecture Notes in Control and Information Sciences*, pages 957–966, Antibes, France, 1990. Berlin, Germany: Springer-Verlag.
- [16] S. Gaubert. *Théorie des Systèmes Linéaires dans les Dioïdes*. PhD thesis, Ecole Nationale Supérieure des Mines de Paris, France, July 1992.
- [17] S. Gaubert. Timed automata and discrete event systems. In *Proc. of the 2nd European Control Conf.*, pages 2175–2180, Groningen, The Netherlands, June 1993.
- [18] S. Gaubert. On rational series in one variable over certain dioids. Technical Report 2162, INRIA, Le Chesnay, France, January 1994.
- [19] S. Gaubert and J. Mairesse. Task resource models and $(\max,+)$ automata. In J. Gunawardena, editor, *Idempotency*. Cambridge University Press, 1998.
- [20] S. Gaubert and M. Plus. Methods and applications of $(\max,+)$ linear algebra. In *Proc. of the Symp. on Theoretical Aspects of Computer Science*, pages 261–282, Aachen, Germany, 1997.

- [21] B. Giffler. Mathematical solution of production planning and scheduling problems. Technical report, IBM ASDD, October 1960.
- [22] B. Giffler. Scheduling general production systems using schedule algebra. *Naval Research Logistics Quarterly*, 10(3):237–255, September 1963.
- [23] B. Giffler. Schedule algebra: A progress report. *Naval Research Logistics Quarterly*, 15(2):255–280, June 1968.
- [24] M. Gondran and M. Minoux. Eigenvalues and eigenvectors in semimodules and their interpretation in graph theory. In *Proc. of the 9th Int. Mathematical Programming Symp.*, pages 333–348, Budapest, Hungary, August 1976.
- [25] M. Gondran and M. Minoux. Linear algebra in dioids: A survey of recent results. *Annals of Discrete Mathematics*, 19:147–163, 1984.
- [26] M. Gondran and M. Minoux. Dioïd theory and its applications. In *Algèbres Exotiques et Systèmes à Événements Discrets, CNRS/CNET/INRIA Seminar*, pages 57–75, CNET, Issy-les-Moulineaux, France, June 1987.
- [27] S. Grillner. Neurobiological bases of rhythmic motor acts in vertebrates. *Science*, 228(4696):143–149, 1985.
- [28] S. Grillner. Control of locomotion in bipeds, tetrapods, and fish. *Comprehensive Physiology*, Supplement 2: Handbook of Physiology, The Nervous System, Motor Control:1179–1236, 2011.
- [29] G.C. Haynes, F.R. Cohen, and D.E. Koditschek. Gait transitions for quasi-static hexapedal locomotion on level ground. In *Proc. of the Int. Symp. of Robotics Research*, pages 105–121, Lucerne, Switzerland, 2009.
- [30] B. Heidergott. A characterisation of $(\max,+)$ -linear queueing systems. *Queueing Systems: Theory and Applications*, 35:237–262, 2000.
- [31] B. Heidergott and R. de Vries. Towards a $(\max,+)$ control theory for public transportation networks. *Discrete Event Dynamic Systems*, 11:371–398, 2001.
- [32] B. Heidergott, G. Olsder, and J. van der Woude. *Max Plus at Work: Modeling and Analysis of Synchronized Systems*. Kluwer, 2006.
- [33] M. Hildebrand. Symmetrical gaits of horses. *Science*, 150(3697):701–708, 1965.
- [34] P. Holmes, R. Full, D.E. Koditschek, and J. Guckenheimer. The dynamics of legged locomotion: models, analyses, and challenges. *SIAM Review*, 48(2):207–304, 2006.
- [35] A.J. Ijspeert. Central pattern generators for locomotion control in animals and robots: A review. *Neural Networks*, 21(4):642–653, 2008.
- [36] R.M. Karp. A characterization of the minimum cycle mean in a digraph. *Discrete Mathematics*,

23(3):309–311, 1978.

- [37] E. Klavins and D.E. Koditschek. Phase regulation of decentralized cyclic robotic systems. *Int. J. of Robotics Research*, 21(3):257–275, 2002.
- [38] G.A.D. Lopes, R. Babuška, B. De Schutter, and T. van den Boom. Switching max-plus models for legged locomotion. In *Proc. of the IEEE Int. Conf. on Robotics and Biomimetics*, pages 221–226, Guilin, China, 2009.
- [39] G.A.D. Lopes, T. van den Boom, B. De Schutter, and R. Babuška. Modeling and control of legged locomotion via switching max-plus systems. In *Proc. of the Int. Workshop on Discrete Event Systems*, pages 392–397, Berlin, Germany, 2010.
- [40] E. Muybridge. *The Human Figure in Motion*. Dover Publications, 1901.
- [41] G.J. Olsder. On the characteristic equation and minimal realizations for discrete-event dynamic systems. In *Proc. of the 7th Int. Conf. on Analysis and Optimization of Systems*, volume 83 of *Lecture Notes in Control and Information Sciences*, pages 189–201, Antibes, France, 1986.
- [42] G.J. Olsder, J.A.C. Resing, R.E. de Vries, M.S. Keane, and G. Hooghiemstra. Discrete event systems with stochastic processing times. *IEEE Tran. on Automatic Control*, 35(3):299–302, March 1990.
- [43] G.J. Olsder and C. Roos. Cramer and Cayley-Hamilton in the max algebra. *Linear Algebra and Its Applications*, 101:87–108, 1988.
- [44] J.L. Peterson. *Petri Net Theory and the Modeling of Systems*. Englewood Cliffs, New Jersey: Prentice Hall, Inc., 1981.
- [45] M.H. Raibert. *Legged Robots That Balance*. MIT Press, Cambridge, Massachusetts, USA, 1986.
- [46] M.H. Raibert, H.B. Brown Jr., M. Chepponis, J. Koechling, J.K. Hodgins, D. Dustman, W.K. Brennan, D.S. Barrett, C.M. Thompson, J.D. Hebert, W. Lee, and L. Borvansky. Dynamically stable legged locomotion. Technical Report 1179, MIT, 1989.
- [47] U. Saranli, M. Buehler, and D.E. Koditschek. RHex: a simple and highly mobile hexapod robot. *Int. J. of Robotics Research*, 20(7):616–631, 2001.
- [48] K. Shedden. Analysis of cell-cycle gene expression in *Saccharomyces cerevisiae* using microarrays and multiple synchronization methods. *Nucleic Acids Research*, 30(13):2920–2929, July 2002.
- [49] J.D. Weingarten, R.E. Groff, and D.E. Koditschek. A framework for the coordination of legged robot gaits. In *Proc. of the IEEE Conf. on Robotics, Automation and Mechatronics*, pages 679–686, Singapore, 2004.
- [50] S. Yamaguchi. Synchronization of cellular clocks in the suprachiasmatic nucleus. *Science*, 302(5649):1408–1412, 2003.
- [51] M. Zhou, F. DiCesare, and A.A. Desrochers. A hybrid methodology for synthesis of Petri net models

for manufacturing systems. *IEEE Tran. on Robotics and Automation*, 8(3):350–361, June 1992.